

The Genomic Loci of Specific Human tRNA Genes Exhibit Ageing-Related DNA Hypermethylation

Richard J. Acton ¹, ², ³, Wei Yuan ⁴, ⁵, Fei Gao ⁶, Yudong Xia ⁶, Emma Bourne ⁷, Eva Wozniak ⁷, Jordana Bell ⁴, Karen Lillycrop ³, Jun Wang ⁶, Elaine Dennison ², Nicholas Harvey ², Charles A. Mein ⁷, Tim D. Spector ⁴, Pirro G. Hysi ⁴, Cyrus Cooper ², Christopher G. Bell ¹ *

1 William Harvey Research Institute, Barts & The London School of Medicine and Dentistry, Charterhouse Square, Queen Mary University of London, London, U.K.

2 MRC Lifecourse Epidemiology Unit, University of Southampton, Southampton, U.K.

3 Human Development and Health, Institute of Developmental Sciences, University of Southampton, Southampton, U.K.

4 Department of Twin Research & Genetic Epidemiology, St Thomas Hospital, King's College London, London, U.K.

5 Institute of Cancer Research, Sutton, U.K.

6 BGI-Shenzhen, Shenzhen, China

7 Barts & The London Genome Centre, Blizard Institute, Barts & The London School of Medicine and Dentistry, Queen Mary University of London, London, U.K.

* Corresponding author:

c.bell@qmul.ac.uk

1

Abstract

The epigenome has been shown to deteriorate with age, potentially impacting on ageing-related disease. tRNA, while arising from only ~46kb (<0.002% genome), is the second most abundant cellular transcript. tRNAs also control metabolic processes known to affect ageing, through core translational and additional regulatory roles. Here, we interrogate the DNA methylation state of the genomic loci of human tRNA. We identify a genomic enrichment for age-related DNA hypermethylation at tRNA loci. Analysis in 4,350 MeDIP-seq peripheral-blood DNA methylomes (16-82 years), identifies 44 and 21 hypermethylating specific tRNAs at study-and genome-wide significance, respectively, contrasting with 0 hypomethylating. Validation and replication (450k array & independent targeted Bisulphite-sequencing) supported the hypermethylation of this functional unit. Tissue-specificity is a significant driver, although the strongest consistent signals, also independent of major cell-type change, occur in tRNA-iMet-CAT-1-4 and tRNA-Ser-AGA-2-6. This study presents a comprehensive evaluation of the genomic DNA methylation state of human tRNA genes and reveals a discreet hypermethylation with advancing age.

Introduction

Ageing is implicated as a risk factor in multiple chronic diseases [1]. Understanding how the ageing process leads to deteriorating biological function is now a major research focus, with hopes to increase the human ‘healthspan’ and ameliorate the extensive physical, social and economic costs of these ageing-related disorders [2]. Epigenetic processes, which influence or can inform us about cell-type specific gene expression, are altered with age and are, furthermore, one of the fundamental hallmarks of this progression [3,4].

DNA methylation (DNAm) is the most common epigenetic modification of DNA and age-associated changes in this mark in mammalian tissues have been recognised for decades [5]. In fact, these alterations in DNAm with age are extensive with thousands of loci across the genome affected. Many represent ‘drift’ arising from the imperfect maintenance of the epigenetic state [6]. However, specific genomic regions show distinct directional changes, with loss of DNA methylation in repetitive or transposable elements [7], as well as gains in certain promoters, including the targets of polycomb repressor complex [8] and bivalent domains [9]. These observations with the advent of high-throughput DNAm arrays also permitted the identification of individual CpG sites that exhibit consistent changes with age, enabling the construction of predictors of chronological age known as epigenetic or DNAm ‘clocks’ [10–13]. Additionally, it was observed that ‘acceleration’ of this DNAm-derived measure is a biomarker of ‘biological’ ageing due to associations with morbidity and mortality (Reviewed in [14] & [15]). In a previous investigation of ageing-related DNAm changes within common disease-associated GWAS regions, we identified hypermethylation of the specific transfer RNA gene, tRNA-iMet-CAT-1-4 [16]. The initiator methionine tRNA possesses certain unique properties, including its capacity to be rate limiting for translation [17], association with the translation initiation factor eIF2 [18], and ability to impact the expression of other tRNA genes [19].

tRNAs are evolutionarily ancient [20] and fundamental in the translation process for all domains of life. This translation machinery and the regulation of protein synthesis are controlled by conserved signalling pathways shown to be modifiable in longevity and ageing interventions [21]. Additionally, beyond their core role in the information flow from DNA to protein sequence, tRNAs can fragment into numerous tRNA-derived small RNAs (tsRNAs) [22] with signalling and regulatory functions [23–26].

When liberally considering the 610 loci annotated as tRNA genes, as well as tRNA pseudo genes, nuclear encoded mitochondrial tRNA genes and possibly some closely related repetitive sequences, these features (gtRNADB [27]) cover <46 kb (including introns) which represents <0.002% of the human genome [28]. Yet a subset of these genes produce the second most abundant RNA species next to ribosomal RNA [29] and are required for the production of all proteins. tRNA genes are transcribed by RNA polymerase III (polIII) [30] and

have internal type II polIII promoters [31]. DNAm is able to repress the expression of tRNA genes 46 experimentally [32] but may also represent co-ordination with the local repressive chromatin state [33]. 47 Transcription is also repressed by the highly conserved polIII specific transcription factor Maf1 [34,35], who's 48 activity is modulated by the Target of Rapamycin Kinase Complex 1 (TORC1) [36]. TORC1 is a highly 49 conserved hub for signals that modulate ageing [37]. 50

tRNAs as well as tsRNAs are integral to the regulation of protein synthesis and stress response, two processes 51 known to be major modulators of ageing. Metabolic processes are also recognised to modulate the age estimates 52 of DNAm clocks [38]. Partial inhibition of translation increases lifespan in multiple model organisms [39] and 53 PolIII inhibition increases longevity acting downstream of TORC1 [40]. Furthermore, certain tsRNAs circulating 54 in serum can be modulated by ageing and caloric restriction [41]. 55

We directly investigated ageing-related changes in the epigenetic DNA methylation state of the entire tRNA 56 gene set, facilitated by the availability of a large-scale MeDIP-seq dataset. Arrays poorly cover this portion of 57 genome, with even the latest EPIC (850k) arrays only covering <15% of the tRNA genes, with robust probes, and 58 in total only ~4.7% of all the tRNA gene CpGs [42]. tRNA genes sit at the heart not only of the core biological 59 process of translation but at a nexus of signalling networks operating in several different paradigms, from small 60 RNA signalling to large scale chromatin organisation [43]. In summary, tRNA biology, protein synthesis, nutrient 61 sensing, stress response and ageing are all intimately interlinked. In this study, we have identified tRNA gene 62 DNA hypermethylation and independently replicated this newly described ageing-related observation. 63

Results

64

DNA Methylation of Specific tRNA Gene Loci Changes with Age

65

Due to tRNAs critical role in translation and evidence of their modulation in ageing and longevity-related pathways, we interrogated these genes for evidence of ageing-related epigenetic changes. Our discovery set was a large-scale peripheral blood-derived DNA methylome dataset comprising of 4350 samples. This sequencing-based dataset had been generated by Methylated DNA Immunoprecipitation (MeDIP-seq) [44], which relies on the enrichment of methylated fragments of 200-500 bp to give a regional DNAm assessment (500 bp semi-overlapping windows, see Methods). There are 416 high confidence tRNA genes in the human genome, we initially examined an expanded set of 610 tRNA-like features identified by tRNAscan including pseudogenes, possible repetitive elements, and nuclear encoded mitochondrial tRNAs [27,45]. Of these 492 were autosomal and did not reside in blacklisted regions of the genome [46]. Due to the small size of these tRNAs (60-86bp, median 73bp, excluding introns which are present in ~30 tRNAs with sizes from 10-99bp, median 19bp), this fragment-based method enabled a robust examination of the epigenetic state of these highly similar sequences. This was supported by a mappability assessment. The median mappability score density for all tRNA genes was 0.90 for 50mers when considering tRNA genes $\pm 500\text{bp}$ reflecting the regional nature of the MeDIP-seq assay. In contrast the 50mer mappability density is 0.68 for tRNA genes alone, which would be representative of the mappability of reads generated using a technique such as whole-genome bisulfite sequencing (see Supplementary Figure 1 & Supplementary Figure 2).

We identified 21 genome-wide significant and 44 study-wide significant results ($p < 4.34 \times 10^{-9}$ and 8.36×10^{-5} , respectively), via linear regression ($n=4350$, see Methods). Study-wide significance was calculated conservatively with the Bonferroni method for all 598 autosomal tRNAs and closely related features. There was a strong directional trend with all results at both significance levels being due to increases in DNA methylation. Age-related changes in cell type proportion are strong in heterogeneous peripheral blood, and include a myeloid skew, loss of naive T cells and increases in senescent cells [47]. A subset of 3 genome-wide and 16 study-wide significant hypermethylation results remained significant even after correcting for potential cell-type changes by including lymphocytes, monocytes, neutrophils and eosinophil cell count data ($n=3001$, Listed in Figure 1, see Supplementary Figure 3). Going forward we refer to these cell-type corrected sets of 3 and 16 tRNA genes as the genome-wide and study-wide significant tRNA genes respectively.

tRNA	Window	MeDIP		450k Array		Targeted BiS-seq	
		Slope	p-value	Slope	p-value	Slope	p-value
tRNA-Gln-CTG-7-1	Chr1:147,800,750-147,801,250	0.84	2.60e-05				
	Chr2:131,094,500-131,095,000	1.11	4.64e-09				
tRNA-Glu-TTC-1-1	Chr2:131,094,250-131,094,750	1.00	1.12e-07				
	Chr2:131,094,750-131,095,250	1.00	3.28e-07				
tRNA-His-GTG-1-2	Chr1:146,544,500-146,545,000	0.92	1.38e-06				
tRNA-His-GTG-2-1	Chr1:149,155,750-149,156,250	1.05	2.98e-08				
	Chr1:149,155,500-149,156,000	0.83	1.37e-05				
tRNA-Ile-AAT-10-1	Chr6: 27,251,500- 27,252,000	1.07	1.45e-08			1.30	1.22e-03
	Chr6: 27,251,750- 27,252,250	0.90	1.86e-06			1.30	1.22e-03
tRNA-Ile-AAT-4-1	Chr17: 8,130,000- 8,130,500	1.19	2.98e-10	0.20	8.92e-06	-0.74	6.88e-04
	Chr17: 8,130,250- 8,130,750	0.77	3.99e-05	0.20	8.92e-06	-0.74	6.88e-04
tRNA-Ile-TAT-2-2	Chr6: 26,987,750- 26,988,250	0.97	7.25e-07	0.04	1.17e-02	-0.60	3.84e-01
tRNA-iMet-CAT-1-4	Chr6: 26,330,500- 26,331,000	1.28	2.83e-11	0.13	6.07e-06	4.54	9.35e-04
	Chr6: 26,330,250- 26,330,750	1.13	2.89e-09	0.13	6.07e-06	4.54	9.35e-04
tRNA-Leu-TAG-2-1	Chr14: 21,093,250- 21,093,750	1.04	9.38e-08			2.49	8.77e-03
	Chr14: 21,093,500- 21,094,000	0.94	8.50e-07			2.49	8.77e-03
tRNA-Pro-AGG-2-2	Chr6: 26,555,500- 26,556,000	1.04	3.97e-08				
	Chr6: 26,555,250- 26,555,750	1.01	9.58e-08				
tRNA-Ser-ACT-1-1	Chr6: 27,261,250- 27,261,750	0.97	3.53e-07			0.66	1.45e-01
tRNA-Ser-AGA-2-6	Chr17: 8,129,750- 8,130,250	1.21	1.16e-10	0.21	6.72e-05	0.62	4.28e-02
	Chr17: 8,130,000- 8,130,500	1.19	3.03e-10	0.21	6.72e-05	0.62	4.28e-02
tRNA-Ser-TGA-2-1	Chr6: 27,513,000- 27,513,500	0.90	3.58e-06	0.87	1.38e-04	-0.25	5.74e-01
tRNA-Val-AAC-1-2	Chr5:180,590,750-180,591,250	0.91	3.28e-06				
tRNA-Val-AAC-4-1	Chr6: 27,648,500- 27,649,000	1.07	1.25e-08	0.40	9.90e-03		
	Chr6: 27,648,750- 27,649,250	0.95	4.31e-07	0.40	9.90e-03		
tRNA-Val-CAC-2-1	Chr6: 27,247,750- 27,248,250	0.85	2.33e-05	0.59	5.05e-06		

Figure 1. Ageing-related DNA methylation changes in tRNA loci (16 Study-wide significant after blood cell-type correction, $p < 8.36 \times 10^{-5}$). Columns left to right: tRNA gene; Genomic location of MeDIP-seq significant window (hg19); MeDIP results slope (arbitrary units) and p-value; 450k Array results slope (beta) and p-value (Blood-cell corrected and combined for all probes overlapping tRNA); Targeted Bisulphite-sequencing (BiS-seq) slope (model beta) and p value (combined all CpGs in targeted region, see Methods). Units of slope are quantile normalised RPM values or MeDIP-seq models and proportion of CpG sites methylated for the targeted bisulfite and array based assays, all per unit time. Result for all covered tRNAs are included in the (supplementary data 1, 3, & 4). All p-values are for F-tests from simple linear regression. For slope: Orange = hypermethylation and Blue = hypomethylation with age. For p-values: Colour gradient high significance = dark blue to low significance = yellow, scaled relative to column. Blank grey cells indicate unavailable data.

Due to the related nature of these twin samples, we also analysed these data in two subsets of $n = 1198$ & 1206 by selecting one twin from each pair into the separate sets. This analysis also included correction for Blood Cell counts. Even in these smaller sets, 5 and 7 tRNA genes, respectively, reached study-wide significance. In these sets 5/5 and 6/7 of these were present in 16 study-wide significant tRNA genes.

Furthermore, we examined a subset of samples with longitudinal data ($n=658$ methylomes from 329

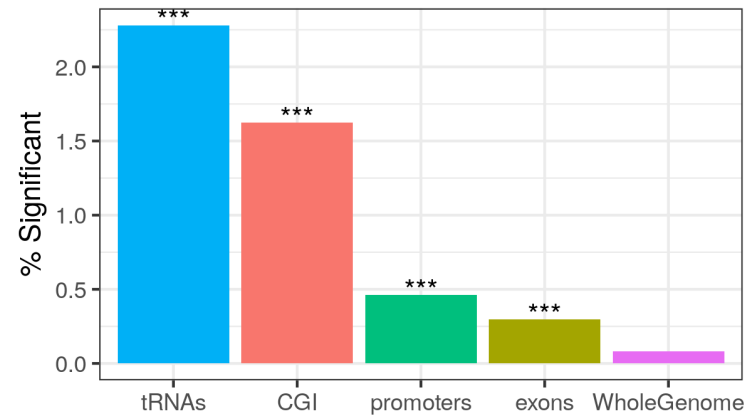
individuals, median age difference 7.6 yrs). At the nominal significance threshold ($p < 0.05$) this yielded a split
97 of 41 hypermethylating tRNA genes and 22 hypomethylating tRNA genes. Of these hypermethylated tRNAs, 2
98 are in the previously identified genome-wide significant set of 3 (with tRNA-iMet-CAT-1-4 ranked 3rd by p-value)
99 and 9 are in the study-wide significant set of 16. We also ran a number of additional analyses to investigate this
100 directional observation further, including performed linear mixed modeling with batch, lymphocyte, monocyte,
101 neutrophil and eosinophil cell count data, as fixed effects, and family id and zygosity as random effects. Thus we
102 have observed the same consistent hypermethylation trend with age across a wide array of models, with and
103 without correction for cell-type composition, and when either correcting for structure in our sample population or
104 when examining those sub-populations separately. Full results for each age model are provided in Supplementary
105 Data 1
106

tRNA Genes are Enriched for Age Related DNA Hypermethylation

107

Whilst ageing changes are pervasive throughout the DNA methylome, we identified a strong enrichment for this
108 to occur within the tRNA genes (Fisher's Exact Test $p = 1.05 \times 10^{-27}$) (see Figure 2 b). This is still significant if
109 the 6 of the study-wide significant 16 tRNAs that have any overlap with polycomb or bivalent regions are
110 excluded ($p = 4.66 \times 10^{-15}$)
111

a Significant Age Related Hypermethylation
 Percentage of significant windows by feature type



b CpG Density Permutation Analysis

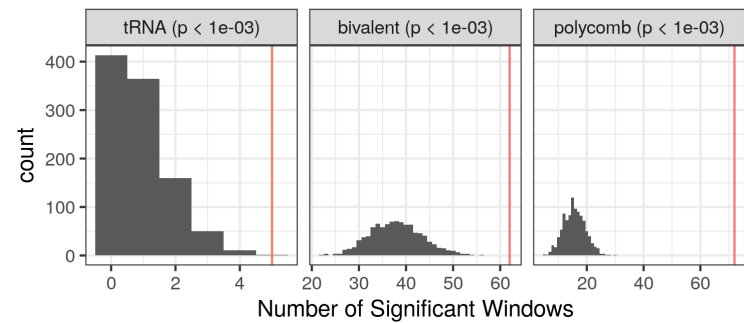


Figure 2. Age-related hypermethylation is enriched in tRNA genes relative to genomic background and accounting for CpG density **A)** tRNA genes are enriched for age-related hypermethylation compared to the genomic background, Fisher's Exact Test $p < 1.05 \times 10^{-27}$, 1-sided). All Fisher's exact test results are included in Supplementary data 2 (CGI) CpG islands. **B)** tRNA genes show more significant hypermethylated loci than CpG Density matched permutations. Each permutation represented a random set of windows matching the CpG density of the functional unit (tRNA gene loci, bivalent domains, and polycomb group target promoters). These are subsequently assessed for significant age-related DNAm changes, quoted p-values are empirical p-values based on the permutation results (see Methods). The red line is the observed number of significant loci. Source data are provided as a Source Data file.

CpG density itself is known to have a clear impact on the potential for variability of the DNA methylome as well as ageing-related changes [48,49]. To assess whether this hypermethylation finding was being merely driven by the inherent CpG density of the tRNA genes, we performed a CpG density matched permutation analysis (1,000X, see Methods). This supported the specific nature of these age-related DNAm changes within the functional tRNA genes (Empirical p -value $< 1.0 \times 10^{-3}$, Figure 2 a). As a point of comparison for this genomic functional unit, we also performed the same permutations for the known age-related changes in the promoters of genes that are polycomb group targets [8] and those with a bivalent chromatin state [9]. We were able to

reproduce the enrichment of the polycomb group targets and bivalent regions (Empirical p-value < 1.0×10^{-3}) in our dataset.

tRNA-iMet-CAT-1-4 (Figure 3a) is located in the largest tRNA gene cluster in the human genome at chr6p22.2-1. This cluster contains 157 tRNA genes spanning the 2.67Mb from tRNA-iMet-CAT-1-2 to tRNA-Leu-AAG-3-1, and also hosts a histone gene microcluster. tRNA-Ile-AAT-4-1 and tRNA-Ser-AGA-2-6 are neighbours and are located on chromosome 17 (Figure 3b). Notably tRNA-Ile-AAT-4-1 and tRNA-Ser-AGA-2-6 have a third close neighbour tRNA-Thr-AGT-1-2 which does not show significant age-related hypermethylation. We observe a similar pattern of sharp peaks of significance closely localised around the other loci in the study-wide significant set. GENCODE 19 places tRNA-Ile-AAT-4-1 in the 3'UTR of a Nonsense-mediated decay transcript of *CTC1* (CST Telomere Replication Complex Component 1, CTC1-201, ENST00000449476.7) and not of its primary transcript.

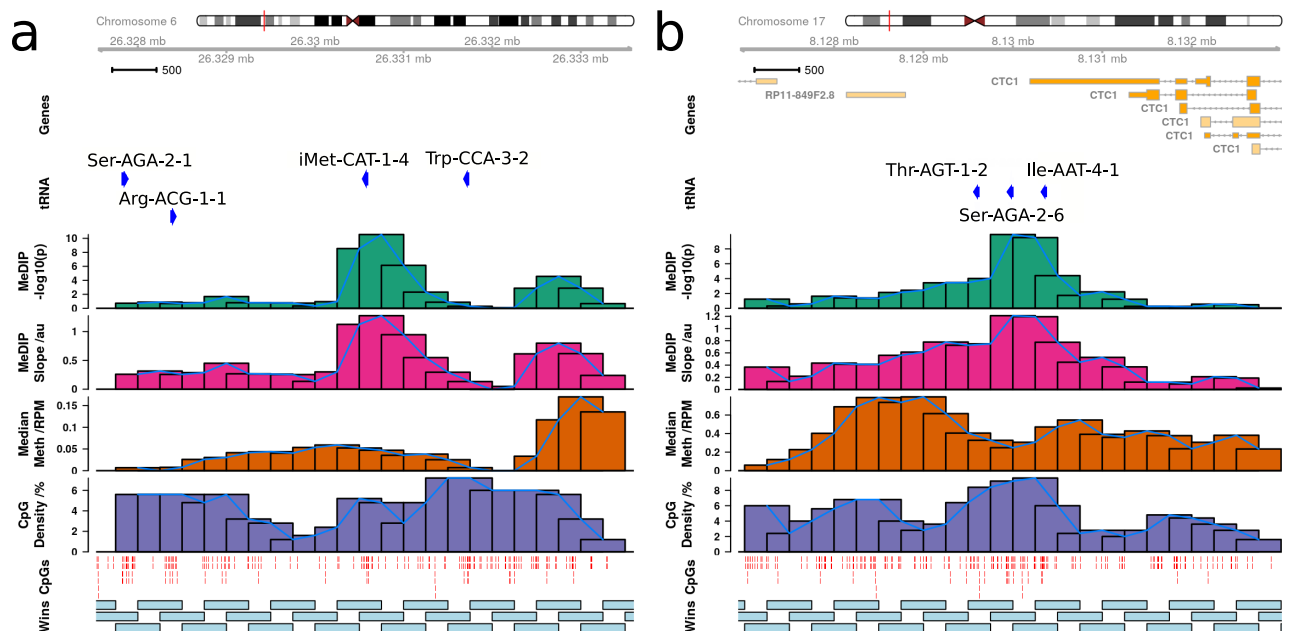


Figure 3. Age-related tRNA gene DNA hypermethylation is localised to individual tRNA genes. MeDIP-seq results (blood cell-type corrected model) for A) tRNA-iMet-CAT-1-4 as well as B) tRNA-Ser-AGA-2-6 and tRNA-Ile-AAT-4-1 exhibiting ageing-related DNA hypermethylation. Top to Bottom: Chromosome ideogram; Gene locations (GENCODE 19); MeDIP-seq DNA methylation ageing $-\log_{10} p$ -value results (shown for each 500 bp overlapping window); MeDIP-seq slope of change with age; MeDIP-seq Medium coverage (Reads per Millions, RPM) calculated across all samples; CpG density (%); CpG locations (red lines); 500bp overlapping windows. The sharp peaks suggest that the results are localised to individual tRNA genes not the entire genic locus. One window overlapping tRNA-Ile-AAT-4-1 also partially overlaps tRNA-Ser-AGA-2-6. The 3' UTR of the CTC1 transcript CTC1-201 (ENST00000449476.7, GENCODE 19), which is subject to nonsense mediated decay, overlaps tRNA-Ile-AAT-4-1. tRNA genes with similar CpG density are exhibiting differing age-related DNAm change patterns. Source data are provided as a Source Data file.

To place these hypermethylating tRNA genes in their genomic context we examined how the extended set of

44 non-blood cell-type corrected study-wide significant tRNAs clustered with other tRNA genes. We clustered the tRNA genes by grouping together all tRNAs within 5Mb of one another and then required that a cluster contain at least 5 tRNA genes with a density of at least 5 tRNA genes per Mb (see Methods). This yielded 12 major tRNA gene clusters containing a total of 353 tRNA genes, 42 of the 44 study-wide significant tRNA genes within these clusters (Figure 4a). The hypermethylating tRNA genes are spread evenly among these clusters proportionately to their size (% ageing tRNA per cluster; non-significant one-way ANOVA).

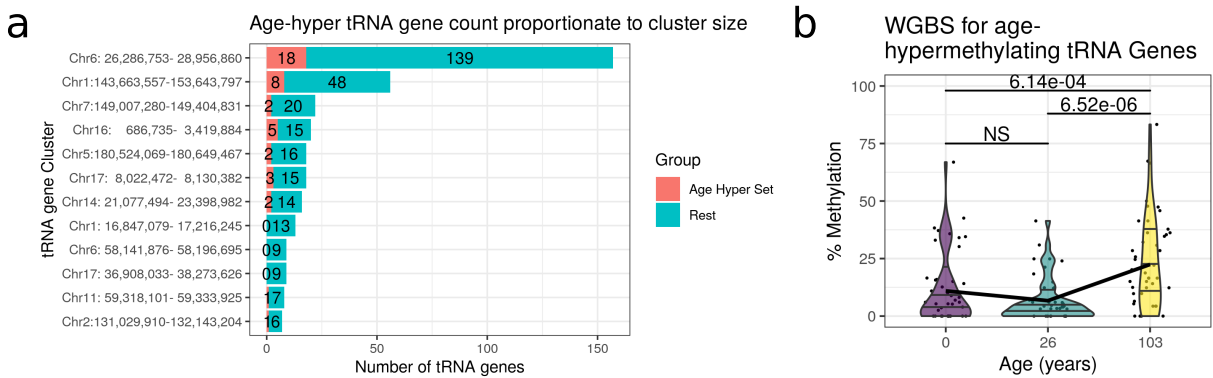


Figure 4. Age-hypermethylation tRNAs Can be Seen When Comparing a Neonate to a Centenarian and are Distributed Proportionately Across Major tRNA Gene Clusters **A)** No significant clusters of ageing-related tRNA. Proportion of non-blood cell corrected ageing-related study-wide significant tRNAs (42/44, red) within tRNA clusters (tRNAs within 5Mb with >5 tRNA genes/Mb, see Methods). **B)** Covered study-wide significant tRNA genes ($n = 14/16$) are more methylated in a centenarian than in a neonate or an adult (26 year) in Whole Genome Bisulfite Sequencing (WGBS) data from Heyn et al. [50]. Each point represents individual CpG methylation levels within a tRNA gene. The horizontal lines in the violin plots represent the 25%, 50% and 75% quantiles. (NS) Not Significant. Source data are provided as a Source Data file.

Age-related tRNA gene set DNA Hypermethylation is even observed in one Newborn versus one Centenarian

We examined an available Whole Genome Bisulphite sequencing (WGBS) dataset from Heyn *et al.* [50] (see Methods) These data consisted of blood-derived DNA WGBS in one newborn child and one 26 year old, and centenarian (103 years). In their analysis, the centenarian was found to have more hypomethylated CpGs than the neonate across all genomic compartments, including promoters, exonic, intronic, and intergenic regions. However, even in this examination of 3 individuals of 3 different ages in the 55% of tRNA genes that possessed coverage, we observed DNA hypermethylation with age among the study-wide significant hypermethylating tRNA genes. The centenarian was significantly more methylated in this set of tRNAs than the neonate (Wilcoxon rank sum test, 6.14% increase (95% CI -Inf - 4.31), $W = 717$, $p = 6.14 \times 10^{-4}$, see Figure 4b).

Age-related Changes Independently Replicated with Targeted Bisulfite Sequencing

In order to further robustly support these-ageing related changes, we attempted to replicate these findings ourselves in an independent ageing dataset. Furthermore, we employed a different technology targeted bisulfite (BiS) sequencing to also further validate the MeDIP-seq-derived results. These data provide individual CpG resolution to identify what may be driving the regional DNAm changes observed, and precise quantitation of the magnitude of change.

We performed this targeted BiS-seq in blood-derived DNA from 8 pools of age-matched individuals at 4 time-points (~4, ~28, ~63, ~78 years) from a total of 190 individuals, as detailed in Table 1. This approach permitted us to assay tRNA gene DNA methylation across a large number of individuals whilst requiring a minimal amount of DNA from each (80-100ng), and costing ~1/24th as much as performing sequencing individually. A total of 79 tRNA loci generated reliable results post-QC (see Methods). These tRNAs covered a total of 458 CpGs with a median of 6 CpGs per tRNA (range 1-9). Median Coverage per site across pools, technical replicates and batches was 679 reads (mean 5902).

Firstly, we ran the 8 Pooled samples on the Illumina EPIC (850k) array to confirm that our pooling approach was applicable for DNAm ageing-related evaluation (Available at: GSE166503). This showed an $R^2 = 0.98$ between pool mean chronological age and Horvath clock DNAm predicted age [11](see Figure 5c). Therefore, this confirmed the utility of our pooling approach. We also used these array derived data to estimate the major blood cell proportions for each of these pools with the Houseman algorithm [51].

Table 1. Summary information on participants in each pool Total of 190 participants in 8 pools, at 4 time points: 4, 28, 63, & 78 years

Pool	Mean Age	Sex	Min Age	Max Age	n
Pool 1	4.07	Male	3.99	4.38	20
Pool 2	4.09	Female	3.99	4.36	20
Pool 3	28.07	Female	25.87	29.80	25
Pool 4	28.23	Female	26.05	30.01	25
Pool 5	63.40	Female	62.80	63.80	25
Pool 6	63.26	Female	62.70	63.70	25
Pool 7	77.96	Female	75.50	80.50	25
Pool 8	77.22	Female	74.40	80.10	25

We noted that individual tRNA loci exhibiting age-related changes in DNAm had duplicate or isodecoder (same anticodon but body sequence variation) sequences in the genome, which despite exact or near sequence identity did not show similar changes. tRNA-iMet-CAT-1-4 for instance is 1 of 8 identical copies in the genome and was the only locus that showed significant changes. The results of pairwise differential methylation tests between age groups for the 6 top tRNAs from the MeDIP-seq models are listed in Table 2. tRNA-iMet-CAT-1-4 shows a pairwise increase of 3.7% from age 4 years to age 78 years.

Table 2. Pairwise Differences in Methylation between Age groups by tRNA p-values are for pairwise methylation differences using a paired student's t-test and combined by tRNA region using a generalisation of Fisher's method as implemented the in **RnBeads v2.0.1 R package** (see Methods)[52].

tRNA	num. CpGs	comparison	p-value	delta
tRNA-Ile-AAT-4-1	8	4 vs. 28	1.518e-01	-0.2
		4 vs. 63	1.774e-01	-0.234
		4 vs. 78	3.060e-01	0.0113
		28 vs. 63	7.152e-01	-0.0334
		28 vs. 78	1.553e-01	0.212
		63 vs. 78	2.057e-01	0.245
tRNA-iMet-CAT-1-4	5	4 vs. 28	8.403e-02	0.0116
		4 vs. 63	1.716e-01	0.0125
		4 vs. 78	1.997e-04*	0.0368
		28 vs. 63	3.943e-01	0.000869
		28 vs. 78	1.724e-02*	0.0252
		63 vs. 78	6.224e-02	0.0243
tRNA-Ser-AGA-2-6	9	4 vs. 28	4.222e-01	0.0573
		4 vs. 63	3.968e-01	0.0274
		4 vs. 78	4.651e-01	0.0423
		28 vs. 63	1.095e-01	-0.0299
		28 vs. 78	2.126e-01	-0.015
		63 vs. 78	2.201e-01	0.0149

Of the 3 top hits in MeDIP-seq, tRNA-iMet-CAT-1-4 (Figure 5a(iii)) and tRNA-Ser-AGA-2-6 (Figure 171
 5a(viii)) exceeded nominal significance (p-values = 9.35×10^{-4} & 4.28×10^{-2} , respectively). However, 172
 tRNA-Ile-AAT-4-1 (Figure 5a(xi)) showed a nominal decrease in DNA methylation with age. tRNA tRNA-Leu-TAG-2-1 173
 from the study-wide significant set also showed nominally significant hypermethylation with age (Figure 174
 5a(xviii)). Also, four of the individual CpGs in tRNA-iMet-CAT-1-4 exhibited nominally significant increases in 175
 DNA methylation with Age (Figure 5b). 176

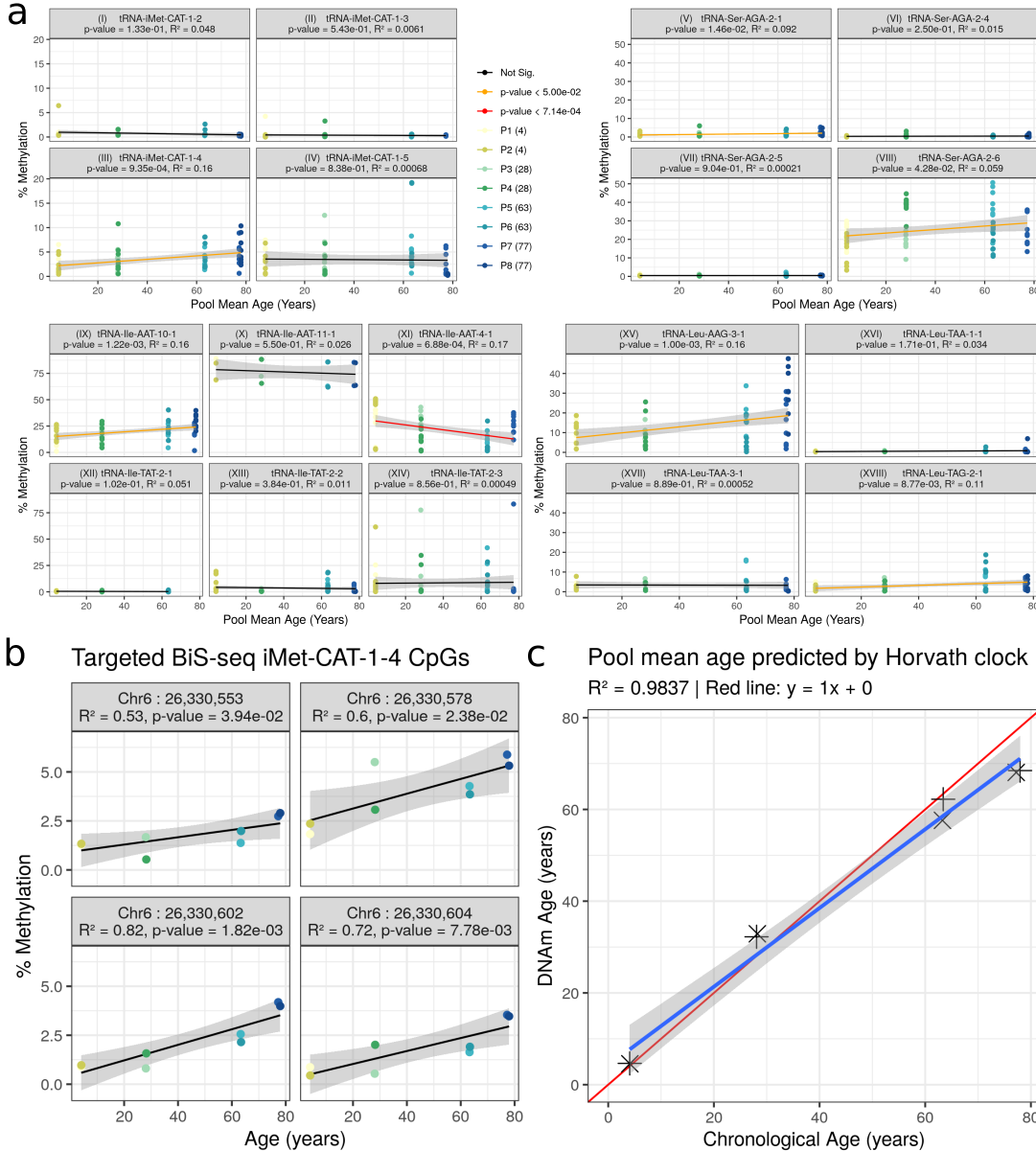


Figure 5. Comparison of Age-related Hypermethylating tRNA Genes to Closely Related tRNA Genes Using Targeted Bisulfite Sequencing (BiS-seq) **A**) Combined CpGs within tRNA loci results (experiment-wide Bonferroni p = 7.14×10^{-4}); *i-iv*, Comparison of select tRNA-iMet-CAT loci: Hypermethylation is specific to iMet-CAT-1-4 (iii) not other isodecoders (i, ii, & iv); *v-viii*, Comparison of select tRNA-Ser-AGA loci: Hypermethylation is specific to Ser-AGA-2-6 A (viii) and to a lesser extent Ser-AGA-2-1 (v), whilst not other isodecoders (vi, vii); *ix-xiv*, Comparison of select tRNA-Ile loci: Hypermethylation is specific to Ile-AAT-10-1 (ix), Ile-AAT-4-1 (xi) displays hypomethylation contrary to previous MeDIP findings, Ile-TAT-2-2 & 2-3 lack hypermethylation (previously non-significant in blood-corrected MeDIP, although significant in uncorrected), whilst no change in Ile-AAT-11-1 (x) and Ile-TAT-2-1 (xii); *xv-xviii*, Comparison of select tRNA-Leu loci: Hypermethylation in Leu-AAG-3-1 (xv) consistent with 450k and Leu-TAG-2-1 (xviii) consistent with MeDIP, whilst no change in Leu-TAA-1-1 (xvi) & Leu-TAA-3-1 (xvii). **B**) tRNA-iMet-CAT-1-4 Individual CpG analysis: 4 CpGs within this tRNA show consistent methylation increases (all p < 0.05). **C**) Mean chronological age is tightly correlated with DNAm Horvath clock [11] predicted age for the 8 pooled samples (see Table 1 for pool details). All p-values are for F-tests from simple linear regression, Error bands represent the SEM. Source data for these plots are provided as a Source Data file and results for all tRNAs covered are provided in supplementary data 3

Select Duplicates & Isodecoders of Hypermethylating tRNA loci remain unchanged We targeted 177 a selection of these duplicate and isodecoder loci for bisulfite sequencing in order to confirm that the identified 178 DNA changes are specific to a given locus and not general to related tRNAs. Examining the tRNA-iMet-CAT-1 179 family, only the previously identified 1-4 version confirmed significant hypermethylation (not 1-2, 1-3 or 180 1-5)(Figure 5a(i-iv)). Likewise the tRNA-Ser-AGA-2-6 version was supported compared to 2-1,2-4 and 2-5(Figure 181 5a(v-viii))). Full Age model results are available in Supplementary Data 8. 182

DNA methylation 450k Array Data Validates the MeDIP-seq Results 183

Although DNA methylation array poorly covers the tRNA gene set, we wished to attempt to see if this BiS-based 184 but differing and well-established technology was supportive at all of our DNA hypermethylation findings. 185 TwinsUK had available 450k array on 587 individuals, and this platform includes 143 probes, covering 103 186 tRNAs. All the 3 top tRNAs in the MeDIP-seq results were covered by this data set, and 7 of the 16 study-wide 187 significant set. 9 tRNAs show significant ($p < 4.58 \times 10^{-4}$) increases in DNA methylation with age in models 188 corrected for blood cell counts including all 3 of the 3 tRNAs identified in the MeDIP-seq as genome-wide 189 significant and 5 of the 7 study-wide significant set present on the array (Figure 6). Although it should be noted 190 that 56 of these 143 probes are within the non-robust set of Zhou et al. [42], including 1 of the genome-wide, and 191 1 of the study-wide results (covering tRNA-Ile-AAT-4-1 & tRNA-Val-AAC-4-1), respectively. Full age model 192 results for all tRNA probes are provided in Supplementary Data 4. 193

Age-related DNA methylation change in tRNA genes

Twins UK – peripheral blood Illumina 450k array

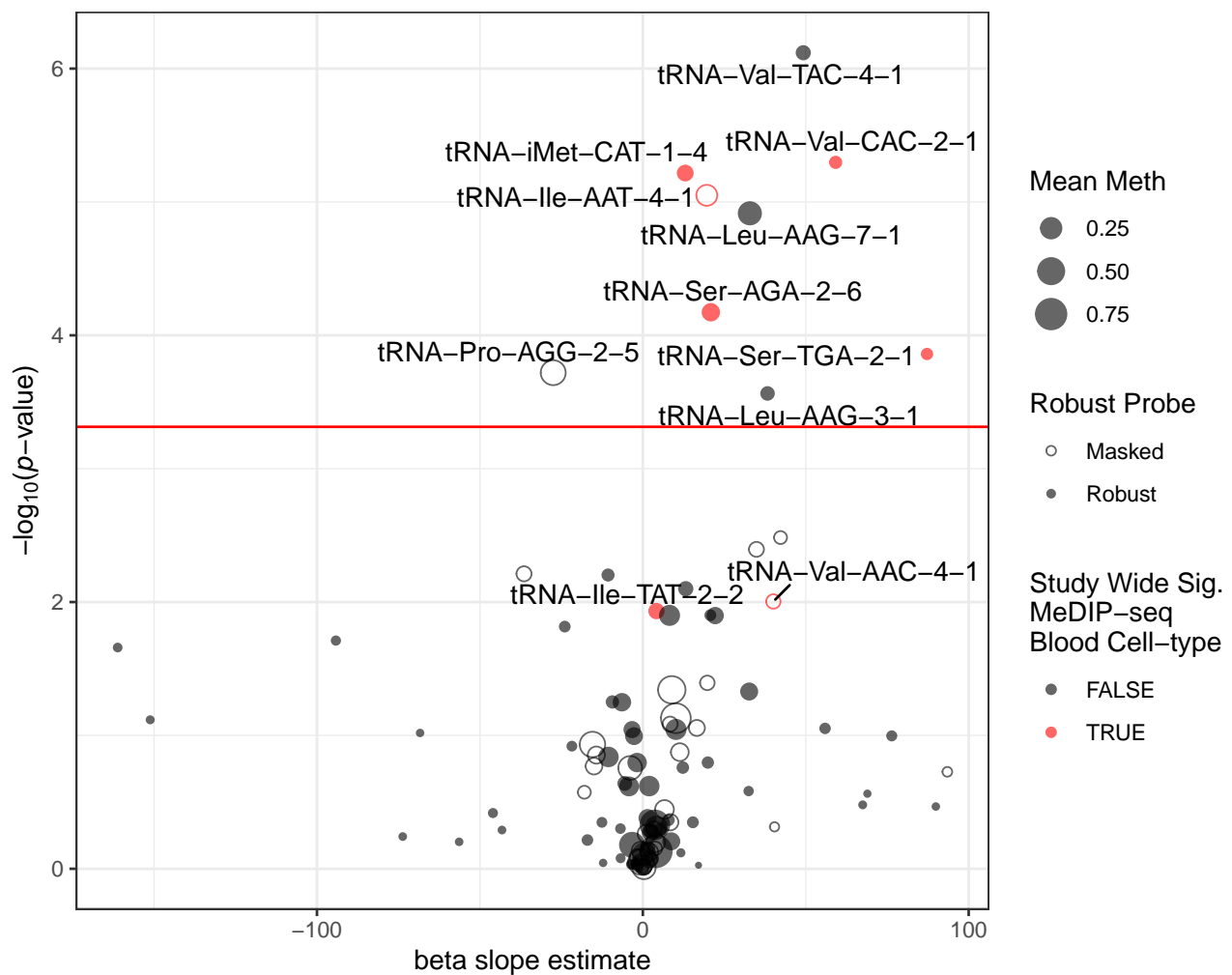


Figure 6. Age-related DNA Methylation Change in tRNA Genes A) Five of seven tRNAs study-wide significant in MeDIP covered by the 450k array also show significant hypermethylation in this data. tRNAs are labelled if they are significant here or were in the MeDIP-seq data (Red). Model slope: the model coefficient for the methylation values. Unfilled circles indicate those probes with potential issues generated by Zhou et al. [42], this includes tRNA-Ile-AAT-4-1. Significance threshold: $0.05/103 \approx 4.58 \times 10^{-4}$ (the number of tRNA genes examined). Source data are provided as a Source Data file. beta = proportion methylated

Ageing-Related tRNA Loci show increased Enhancer-Related Chromatin Signatures

We further explored the activity of the tRNA genes in public Chromatin segmentation data in blood (Epilogs 195 Blood & T-cells set) [53,54]. This shows proportionally more Enhancer-related (Enh, EnhBiv & EnhG) 196 chromatin states at tRNA genes hypermethylating with age than the stronger Promoter-related (TSS) in other 197 tRNAs. (Figure 7 b). Whereas these characteristics are less frequently predominant in the rest of the tRNAs 198 (Figure 7 b). Age-hypermethylating tRNA are enriched for enhancer chromatin states compared to the rest of the 199

tRNA genes (Fisher's Exact test $p = 0.01$). 200

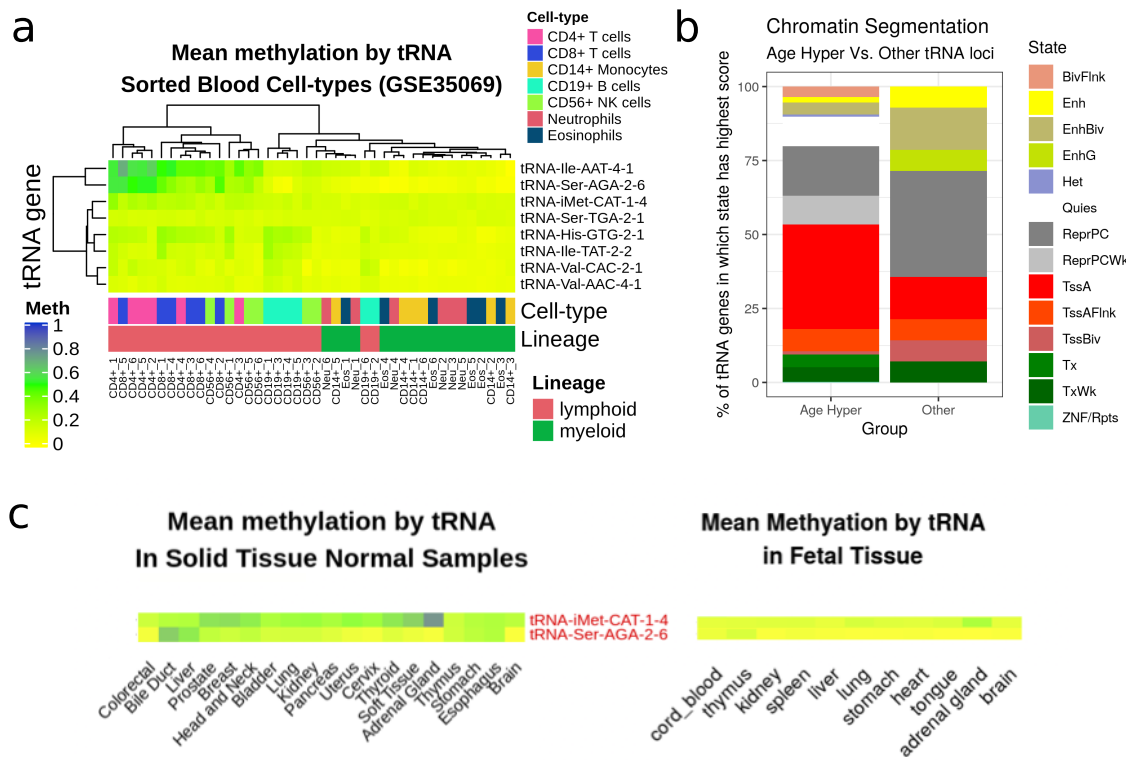


Figure 7. tRNA gene DNA methylation in different blood cell-types **A)** Heatmap of Mean DNA methylation of tRNA sorted Blood Cell Types (data from Reinus et al., probes covering 8 of the 16 study-wide significant tRNA in 7 cell-type fractions from 6 males via GSE35069, [55,56]). This illustrates the ability of tRNA gene methylation to separate the myeloid from the lymphoid lineage and the higher methylation in the lymphoid lineage of the 3 cell-type corrected genome-wide significant tRNAs (iMet-CAT-1-4, etc.) **B)** Chromatin Segmentation data for 'Blood & T-cell' from Epilogos 15 State model [53,54]. Proportion represents the frequency of the predominant chromatin state at a given tRNA (+/- 200bp) for 14/16 study-wide significant tRNAs covered compared to other 371 available tRNAs. The ageing-related hypermethylated tRNAs are enriched for enhancer chromatin state (Fisher's Exact $p = 0.01$). **C)** DNA methylation in 19 tissues from TCGA normal tissue samples and 11 fetal tissues for iMet-CAT-1-4 and Ser-AGA-2-6. Source data are provided as a Source Data file.

Age Hypermethylating tRNAs are more methylated in Lymphoid than Myeloid cells 201

Three tRNA genes remained genome-wide significant and 16 study-wide significant following correction for major cell-type fraction. This is suggestive of either cell-type independent change or, presumably less likely, a very large effect in a minor cell-type fraction. tRNAs have exhibited tissue-specific expression [57–59] and blood cell-type populations change with age. Specifically, there is shift to favour the production of cells in the myeloid lineage [47]. These points lead us to examine tRNA gene DNAm in sorted cell populations. We used a publically available 450k array dataset [55]) that has been used in the construction of cell-type specific DNAm references for cell-type fraction prediction using the Houseman algorithm [51] (see Methods). This consists of data from 6 202 cell types, which we used to predict the cell-type fraction of each sample. 203 We then calculated the mean DNAm for each cell type across all samples. 204 We found that the mean DNAm for the lymphoid cell types was significantly higher than the myeloid cell types. 205 This suggests that the tRNAs are more methylated in the lymphoid lineage than the myeloid lineage. 206 We also found that the mean DNAm for the older samples was significantly higher than the younger samples. 207 This suggests that the tRNAs are more methylated in the older samples than the younger samples. 208

individuals (aged 38 ± 13.6 /yrs) from seven isolated cell populations (CD4+ T cells, CD8+ T cells, CD56+ NK cells, CD19+ B cells, CD14+ monocytes, neutrophils, and eosinophils). We found that tRNA gene DNAm could separate myeloid from lymphoid lineages (Figures 7 a & Supplementary Figure 4).

Of the eight study-wide significant tRNAs with array coverage, we identified that collectively these eight are significantly more methylated in the lymphoid than the myeloid lineage (1.1% difference, Wilcoxon rank sum test $p = 1.50 \times 10^{-6}$ 95% CI 0.7%– ∞). Thus, any age related increases in myeloid cell proportion would be expected to dampen rather than exaggerate the age-related hypermethylation signal that we observed. In addition tRNA-Ile-AAT-4-1 and tRNA-Ser-AGA-2-6 have the highest variance in their DNAm of all 129 tRNAs covered in this dataset. This could represent ageing-related changes as these samples range across almost 3 decades. Another possibility may be that these loci as well as hypermethylating are also increasing their variability with age in a similar fashion to those identified by Slieker *et al.* [60]. In that study they identified that those loci accruing methylomic variability were associated with fundamental ageing mechanisms.

tRNA Genes also Hypermethylate with Age in Solid Tissue

Some tRNA gene expression has been shown to be highly tissue specific [57–59]. It follows that our observations of changes in DNAm with age in blood might be specific to that tissue. We used a mix of 450k and 27k array data from ‘solid tissue normal’ samples made available by TCGA (The Cancer Genome Atlas) and data from foetal tissue [61,62] downloaded from GEO (see Methods). The samples from TCGA range in age from 15–90 ($n = 733$). Only 43 tRNA genes had adequate data to compare across tissues in this dataset and 115 in the foetal tissue data.

Only 2 of the 3 tRNA genes we identified as genome-wide significant and a further 1 of the study-wide significant tRNA genes are present in the set of 45 tRNA genes in the TCGA data, thus limiting our ability to draw conclusions about the tissue specificity of our results. Solid tissue samples have a strong preponderance for low levels of methylation consistent with the active transcription of many tRNA genes and show slight increasing methylation with age but age accounts for very little of the variance (linear regression slope estimate = 1.52; $R^2 = 0.0002$; p-value 1.34×10^{-3} Supplementary Figure 5d). In a pan-tissue analysis we found that 10 tRNA genes showed changes in DNAm with age, 9 of which were hypermethylation (p-value $< 1.1 \times 10^{-3}$). One of these tRNA genes, tRNA-Ser-TGA-2-1 was also present in study-wide significant set of tRNA genes. Supplementary Figure 6 & Supplementary Figure 7 illustrate minimal tissue specific differences. Interestingly, however, tRNA-iMet-CAT-1-4 and tRNA-Ser-AGA-2-6 appeared more variable in methylation state than many other tRNAs in the TCGA normal tissue samples (Supplementary Figure 6) and indeed have the highest variance

in DNA methylation across tissues (Supplementary Figure 5c). These two tRNAs do show broad age-related
239
hypermethylation across a range of tissues in a comparison between fetal to adult, with interestingly,
240
directionally consistent but higher levels for tRNA-iMet-CAT1-4 in the adrenal gland (Figure 7c).
241

Mice also show age-related tRNA gene DNA hypermethylation

242

We examined the DNA methylation of the mouse tRNA genes in using data from a reduced representation
243
bisulfite sequencing (RRBS) experiment performed by Petkovich et al. [63]. These data from 152 mice covered 51
244
tRNA genes and 385 CpGs after QC (see Methods), representing ~11% of mouse tRNA genes. The mice ranged
245
in age from 0.67-35 months.
246

Three of the 51 tRNAs showed Bonferroni significant DNA methylation changes with age (p-value <
247
 1.08×10^{-4}) and all were in the hypermethylation direction. These three are tRNA-Asp-GTC-1-12,
248
tRNA-Ile-AAT-1-4, tRNA-Glu-TTC-1-3 (Figure 8). Full Age model Results are available in Supplementary Data
249
5.
250

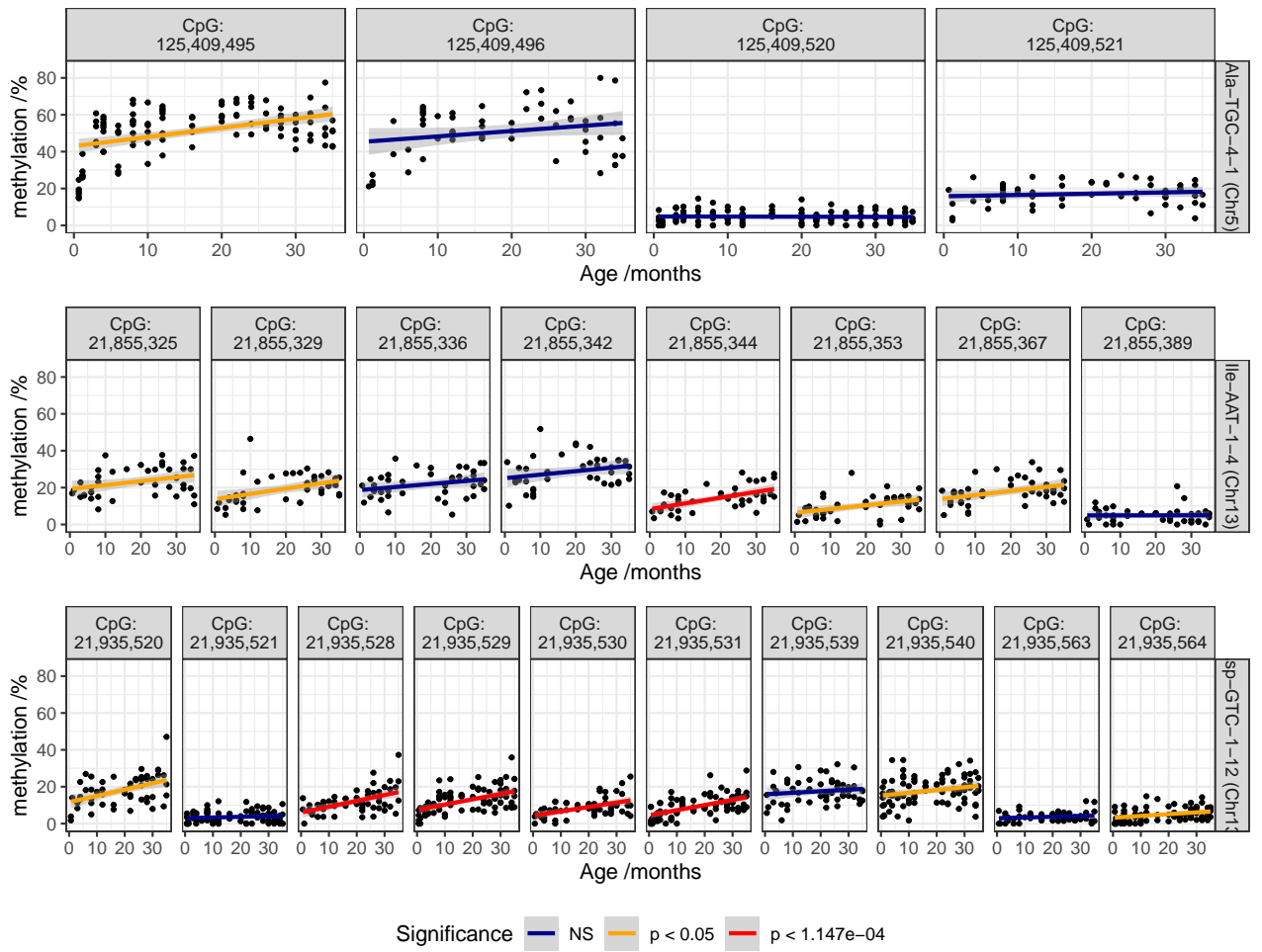


Figure 8. DNA Methylation of CpGs in 3 tRNA Genes Which Significantly Hypermethylate With Age in Mice Data from Petkovich et al. [63]. 6 CpGs reach bonferroni significance and 7 show nominally significant increases. Source data are provided as a Source Data file.

In order to investigate the mouse results further we made use of data from Thornlow et al. [64], which had established tRNA ortholog sets for 29 mammalian species. They identified 197 mouse tRNAs as having direct human orthologs with 44 of these included in the mouse results from Petkovich et al. [63]. However, unfortunately, although 2 of the top 3 tRNAs (tRNA-Ser-AGA-2-6 & tRNA-Ile-AAT-4-1) have mouse orthologs (tRNA-Ser-AGA-2-2 & tRNA-Ile-AAT-1-1), they are not covered in these mouse data. Furthermore, none of the tRNAs showing significant hypermethylation in mice (at nominal $p < 0.05$) had human orthologs in our MeDIP-seq study-wide significant hypermethylating set. Therefore, whilst we cannot directly compare specific tRNA loci due to this lack of coverage, it is interesting that the small number of significant tRNA genes in the mouse data also hypermethylate with age.

Discussion

Our work has identified a previously unknown enrichment for age-related epigenetic changes within the tRNA genes of the human genome. This observation was strongly directional with increasing DNA methylation with age [65]. The MeDIP-seq dataset employed brought advantages in exploring this undefined terrain of the human tRNA genes. Firstly, being genome-wide it provides much increased access, as these regions are poorly covered by current arrays. Secondly, being a fragment-based regional assessment of DNA methylation, the individual but highly similar small tRNA genes can be surrounded by unique sequence.

We determined by genome-wide permutation that this strong hypermethylation signal was specific to the tRNA genes, and not merely driven by the underlying CpG density of these loci. A targeted BiS-seq experiment validated the defined nature of the tRNA change in an independent dataset, with a successful pooling approach, which may also be useful for other ageing-related targeted DNA methylome evaluations. Additionally, we gained support for our results from limited DNA methylation array data.

Whilst the changes in DNA methylation we have observed are relatively small (i.e. 3.7% between 4-year to 78-year pools in tRNA-iMet-CAT-1-4), this is consistent with the effect size seen in the majority of positions differentially methylated with age in many other studies [60,66], except for the noted extreme outliers, such as *EVOLV2* [67]. Furthermore, effect size cut-offs are observed to remove a large fraction of true age-DMPs [68].

We subsequently explored further what was driving this age-related phenomenon and its possible biological implications. As this result was observed in peripheral blood, we were well aware that we were examining DNA derived from a heterogeneous cell type population [69]. Moreover, that there are well known age-related proportional changes in peripheral blood cell composition [47]. The TwinsUK MeDIP-seq and 450k array DNA methylation data included measured haematological values. Therefore, we adjusted for major cell type effects, such as a myeloid skew, and distinct tRNAs were still significant. Although, a caveat to our study is that this can not exclude changes in minor specific sub-cell fractions types. However, that these age-related effects were strong enough to be observed in both a regional MeDIP-seq assessment and a pooled sequencing approach, implies that they not extremely subtle. We examined age-related tRNA gene DNA methylation changes in the limited subset of mouse tRNA genes covered in publicly available RRBS data (~13%) and were able to identify tRNAs exhibiting DNA hypermethylation with age in this set. This suggests that age-related tRNA gene hypermethylation may not be unique to humans, but at least observed across mammals.

Due to the high number of hypermethylating tRNAs prior to cell-type correction, we were also curious whether the epigenetic state of this small tRNA gene fraction of genome could capture and in fact be a defined fingerprint of cell type. We found that tRNA gene DNA methylation could separate myeloid from lymphoid lineages. There

was also some suggestion of more fine-grained blood cell-type signatures in tRNA DNA, such as the separation
291 of CD19+ B cells from CD4/8+ T cells. Ageing is also known to lead to an increase in senescent cells (*e.g.* CD8+
292 CD28- cells). Whether these epigenetic changes in the tRNA genes uniquely represent these cell-types will
293 require technical advances to enable future single cell DNA methylome analysis to accurately assess these regions.
294 If further supported, the epigenetic state of these tRNA loci may aid the taxonomy of cell-type definition.
295

We observed a predominantly unmethylated state across fetal (Supplementary Figure 7) and adult tissues
296 (Supplementary Figure 6) at tRNA gene loci, consistent with the high rate of transcription at many tRNA genes.
297 We suspect that the tRNA genes largely remain unmethylated through development and that the moderate
298 increases in DNA that we are observing with age at these loci are being driven by changes arising primarily in
299 older individuals. Distinct biological changes have been observed recently in aged individuals [70,71]. Our data
300 are supportive of the tRNA gene set representing a distinct functional unit, which lacks the logarithm change in
301 the young observed strongly in CpGs employed in ‘clocks’ [13]. This would also be consistent with the lack of
302 significant differences in the tRNA loci detected between the neonate and the 26-year-old adult in the Heyn et
303 al. data. This low baseline DNA methylation of the tRNA genes may also explain why we predominantly observe
304 hypermethylation with age. Whether this is driven by mechanisms, such as aberrant DNA methylation targeting
305 of the tRNA loci or specific sub-celltype effects with age, will require further experimental investigation.
306

This signal within the tRNA families was observed to occur at specific Isodecoders. Isodecoders expand in
307 number with organismal complexity and the high prevalence in mammals has been suggested due to their
308 additional regulatory functionality [72,73]. They also have distinct translational efficiency [74], which can also
309 have consequences in human disease [75]. After correcting for major cell types, we identified 2 tRNA genes
310 tRNA-iMet-CAT-1-4 and tRNA-Ser-AGA-2-6 which had the most consistent hypermethylation across 3 different
311 assays. Regarding the inconsistent tRNA-Ile-AAT-4-1 result, it is covered by a MeDIP-seq 500bp window which
312 exhibited genome-wide significant hypermethylation, but also partially overlaps tRNA-Ser-AGA-2-6 (Figure 3B).
313 Whilst the 450k array probe overlapping tRNA-Ile-AAT-4-1 (cg06382303) appears to replicate this
314 hypermethylation, it is a borderline case for exclusion flagged by Zhou et al. [42] due to non-unique 30bp 3'
315 subsequence. In the targeted Bisulfite sequencing data, tRNA-Ile-AAT-4-1 exhibited a loss of methylation. These
316 factors considered together suggest that the result for tRNA-Ile-AAT-4-1 should be regarded as inconclusive.
317 Therefore, this may suggest that the hypermethylation signal observed at this locus in the MeDIP-seq data could
318 have been ‘pulled up’ by the neighbouring tRNA-Ser-AGA-2-6 hypermethylation signal. Of the 16 study-wide
319 significant tRNA genes, only these two of these have a shared significant window, furthermore, in the expanded
320 set of 44 only tRNA-Thr-AGT-1-2 could be similarly affected.
321

Furthermore, there is great complexity to the fragmentation of tRNA [23], with physiological processes such
322

as stress shown to induce fragment production [76]. These resultant tsRNAs can feedback on protein synthesis by regulating ribosome biogenesis [77] and others have diverse regulatory functions such as targeting transposable element transcripts [78]. They are also observed to circulate in the blood in a cell-free fashion, and fragment levels can be modulated by ageing and calorie restriction [41]. The isodecoder specific nature of our findings frame a possible hypothesis for regulatory change with age and future work will be required to unravel this potential. tsRNA abundance has been associated with locus specific tRNA gene expression, in some cases independent of mature tRNA levels [79]. This has important implications for the interpretation of our results given the multi-copy nature of genes like tRNA-iMet-CAT-1-4, as even if expression levels of mature iMet tRNAs are unaffected by changes in one copy's DNA methylation, these changes could still influence the levels of particular tsRNAs derived from specific tRNA loci.

The location of tRNA-Ser-AGA-2-6 and tRNA-Ile-AAT-4-1 immediately downstream of *CTC1* and of tRNA-Ile-AAT-4-1 within the 3'UTR of an alternate isoform of *CTC1*, which undergoes nonsense-mediated decay, raises the possibility that the gene body epigenetic regulation of *CTC1* may impact on the state of these tRNA genes. *CTC1*'s function in telomere maintenance [80], DNA replication licensing [81], and it's role in a rare progeroid condition [82] indicate that it has ageing-relevant biology. The possible relationship between the regulation of *CTC1* and that of the tRNA genes downstream of it warrants further study.

Whilst, the expression of the tRNA genes has long been simplified as 'constitutive,' some observations have indicated that many tRNA genes are expressed in a tissue-specific fashion in diverse organisms [58,59]. Although others have found the majority of isodecoders are transcribed in different cell types [28]. Several transcription factors acting via TFIIIB [83] have a negative (the tumour suppressors p53 [84] and Rb [85]) or positive (the proto-oncogene c-Myc) influence [83]. Regulatory sequence in the flanking or the internal regions of tRNA genes do not explain tRNA expression variation [86]. Whilst DNAm is able to repress the expression of tRNA genes [32], the broader chromatin environment also affects tRNA transcription. Due to the co-ordinated nature of epigenomic modifications, it may also be revealing to evaluate ageing-related histone modification in these tRNA loci. Furthermore, recent data from Gerber et al [87] indicates Pol-II may also have a dynamic regulatory role in tRNA expression.

Changes in the epigenetic state of specific tRNA could be modulating transcription efficiency or even codon availability in the ageing cell. tRNA gene dosage is quite closely matched to amino acid usage frequency in the human exome. However, the transcriptome codon usage frequency and tRNA gene expression have been claimed to vary with the replicative state of cells, separating differentiated from replicating cells [88]. Others have argued that these differences are substantially explained by variation in GC content [89] and that codon usage frequencies are observed to be mostly invariant in the transcriptomes of a wide range of tissues, as well as across

developmental time [86]. Although, experimental stress-related states have revealed changes with an over-representation of codons that are translated by rare tRNAs [90].

tRNA sequences themselves are under strong structural (both secondary and tertiary) [72] as well as functional constraint, which leads to an order of magnitude reduction in variation compared the background genomic mutation rate [28]. Despite strong purifying selection maintaining very low variation in tRNA gene bodies, tRNA genes are subject to high levels of transcription-associated mutagenesis (TAM) leading to elevated mutation rates over evolutionary time in their immediate flanking sequences [91]. The possible effects of genetic variation on DNA methylation mean that polymorphic tRNA could be another potential caveat to our work. Although, there is no significant population variation in, for example, tRNA iMet sequences in 1,000 Genomes data. Indeed, there are only 11 new isodecoder sequences with high confidence (tRNAscan scores ≥ 50) at $>1\%$ population frequency [28]. There is also some evidence for tRNA copy number variation at specific loci, although this remains under-characterised [92,93]. Another potential cause we considered was whether age-related somatic copy number increases could be occurring in these loci. Population or somatic copy number expansions could lead to increased methylated reads in MeDIP-seq without any epigenetic state change. However, this would not be consistent with the targeted and array BiS conversion methodologies, where the proportion of methylated to unmethylated reads would still be constant.

It is worth noting the parallels with known cancer and ageing epigenetic changes, and that tRNAs are also dysregulated in cancer [94], with proposed utility as prognostic markers [95]. Furthermore, the early replicating state of tRNA loci, potentially associated with high expression [96], may make them prone to hypermethylate, as is observed in early replicating loci in both cancer [97] and senescent cells [98]. Interestingly, tRNA gene loci may also play a role in local as well as large scale genome organisation [43,99]. tRNA gene clusters act as insulators [100] and have extensive long-range chromatin interactions with other tRNA gene loci [43]. The coordinated transcription of tRNAs at subnuclear foci and the B-box sequence elements bound by TFIIIC and not PolIII may represent an organising principle for 3D-chromatin by providing spatial constraints [101]. Therefore, these tRNA epigenetic changes could contribute to the structural changes that are also observed in ageing [102].

In conclusion, due to the unique challenges that make the tRNA genes difficult to examine it has remained epigenetically under-characterised despite its critical importance for cell function. We directly interrogated the epigenetic DNA methylation state of the functionally important tRNA genes, across the age spectrum in a range of datasets as well as methodologies and identified an enrichment for age-related DNA hypermethylation in the human tRNA genes.

Methods

385

Participants

386

Participants in the ‘EpiTwins’ study are adult volunteers from the TwinsUK Register. The participants were aged between 16 and 82 years, with a median of ~55 years (cohort profile [103]). Ethics for the collection of these data were approved by Guy’s & St Thomas’ NHS Foundation Trust Ethics Committee (EC04/015—15-Mar-04) and written informed consent was obtained from all participants.

390

Participants for our targeted bisulfite sequencing of select tRNA loci were drawn from two studies. Samples from participants aged 4 and 28 years are from the MAVIDOS [104] study and participants aged 63 and 78 years are from the Hertfordshire cohort study [105]. Due to a limited number of available samples, the two 4 year old pools contained DNA from 20 individuals each, with all other pools having 25 contributing individuals. Pool 1, the first 4 year old pool used DNA from all male samples, with all other pools using all female samples. Thus, the total number of participants was 190 (see Table 1). Samples from the 28 year old time point are all from pregnant women at ~11 weeks gestation.

397

tRNA annotation information

398

Genomic coordinates of the tRNA genes were downloaded from GtRNAdb [27]. The 2 tRNAs located in chr1_gl000192_random are tRNA-Gly-CCC-8-1 & tRNA-Asn-ATT-1-2 (Supplementary Data 6). The 213 probes overlapping tRNA genes were derived from intersecting the tRNA gene annotation data from gtRNAdb with the Illumina 450k array manifest annotation for the hg19 genome build using `bedtools` v2.17.0 [106]. We excluded 107 tRNAs from blacklisted regions of hg19 [46].

403

tRNA Gene Clustering

404

We clustered the tRNA genes by grouping together all tRNAs within 5Mb of one another using the `bedtools merge` tool v2.17.0 [106]. We used a command of the form: `bedtools merge -c 4 -o collapse -d N -i hg19-tRNAs.bed` where `N` is the binsize. We varied the binsize and selected 5Mb as it is at approximately this size that number of clusters with more than one tRNAs exceeds the number of singleton tRNAs (Figure Supplementary Figure 9). We added the further requirements that these groupings contain at least 5 tRNA genes with a density of at least 5 tRNA genes per Mb to be considered as clusters.

410

DNA methylome data

411

TwinsUK MeDIP-seq methylomes

412

The Methylated DNA Immunoprecipitation sequencing (MeDIP-seq) data was processed as previously described [16,107]. These processed data are available from the European Genome-phenome Archive (EGA) (<https://www.ebi.ac.uk/ega>) under study number EGAS00001001910 and dataset EGAD00010000983. The dataset used in this work consists of 4350 whole blood methylomes with age data. 4054 are female and 270 male. 3001 have full blood counts. There are 3652 individuals in this data set. These individuals originate from 1933 unique families. There are 1234 monozygotic (MZ) twin pairs (2468 individuals), and 458 dizygotic (DZ) twin pairs (916 individuals).

413

414

415

416

417

418

419

MeDIP-seq used a monoclonal anti-5mC antibody to bind denatured fragmented genomic DNA at methylated CpG sites. The kit used was the ‘MagMeDIP’ kit (Kit Cat. No.: CO2010021 mc-magme-048 from Diagenode

420

421

422

423

(Liège, Belgium) <https://www.diagenode.com/en/p/magmedip-kit-x48-48-rxns>), and the monoclonal antibody

424

was antibody 33D3 (C15200081

425

<https://www.diagenode.com/en/p/5-mc-monoclonal-antibody-33d3-premium-100-ug-50-ul>). The antibody was

426

incubated with Adaptor-ligated DNA combining 0.5µl antibody + 0.5µl water; then 0.6µl MagBuffer A, 1.4µl

427

water and, 2µl MagBuffer C; yielding a final volume of 5µl for the immunoprecipitation reaction. Validation

428

information including for the use of this antibody in MeDIP is provided on the manufacturer’s website in the

429

datasheet for this antibody (

430

https://www.diagenode.com/files/products/antibodies/Datasheet_5-mC33D3_C15200081-100.pdf) This

431

antibody-bound fraction of DNA was isolated and sequenced [44]. MeDIP-seq 50-bp single-end sequencing reads

432

were aligned to the hg19/GRCh37 assembly of the human genome and duplicates were removed. MEDIPS (v1.0)

433

was used for the MeDIP-seq specific analysis [108]. This produced reads per million base pairs (RPM) values

434

binned into 500bp windows with a 250bp slide in the BED format, resulting in ~12.8 million windows on the

435

genome. Thus all individual tRNA genes are covered by 2-3 windows. tRNAs were considered significant if any

436

window overlapping them showed significant changes. MeDIP-seq data from regions of interest was extracted

437

using Bedtools v2.17.0 [106].

438

Analysis of DNA methylome data for Significant Ageing-related changes

439

All analysis was performed in R/3.5.2. Linear models were fitted to age using the MeDIP-seq DNA methylome

440

data, as quantile normalised RPM scores at each 500bp window. Models were fitted with: 1. No covariates; 2.

441

Batch information as a fixed effect; 3. Blood cell-type counts for neutrophils, monocytes, eosinophils, and

442

lymphocytes as fixed effects; and 4. Batch and Blood Cell counts as fixed effects. Model 1 & 2 were fitted on the
441 full set of 4350 as batch information was available for all samples but blood cell count data was only available for
442 a subset of 3001 methylomes. Models 1 & 2 fitted in the n=3001 subset were similar to those fitted in the
443 complete set of 4350. Models 3 & 4 were fitted in the n=3001 subset with full covariate information and sets of
444 significant tRNAs identified at study-wide and genome wide levels in model 4 were used in subsequent analyses.
445 Models were also fitted for two unrelated subsets created by selecting one twin from each pair (Monozygotic or
446 Dizygotic), yeilding sets with n = 1198 & 1206 DNA methylomes. An additional model was fitted for
447 longitudinal analysis, samples were selected by identifying individuals with a DNA methylome at more than one
448 time point and filtering for only those with a minimum of 5 years between samples. This yielded 658 methylomes
449 from 329 individuals with age differences of 5-16.1 yrs, median 7.6 yrs. Models for this set included participant
450 identifier as a fixed effect in addition to blood cell counts and batch information. A mixed effects model was also
451 fit to include the effect of family structure and zygosity (n = 2989). The null model included batch, lymphocyte,
452 monocyte, neutrophil and eosinophil cell count data, as fixed effects, and family id and zygosity as random
453 effects, and was compared to the same model with the addition of the quantile normalised methylation score
454 using anova, mixed models were fit with `lme4 v1.1.21`
455

Permutation Analysis for Enrichment with Age-related Changes

456

We performed a permutation analysis to determine whether the CpG distribution of sets of the tRNA genes was
457 the principle driver of the ageing-related changes observed. Windows overlapping tRNAs have a higher
458 proportion of windows with a greater CpG density than their surrounding sequences (see Supplementary Figure
459 8). CpGs residing within moderate CpG density loci are the most dynamic in the genome [48] and CpG dense
460 CpG island regions include specific ageing-related changes [8,9,16]. For comparison we also performed the
461 permutation in the CGI regions from the Polycomb group protein target promoters in Teschendorff *et al.* [8] and
462 bivalent loci from ENCODE ChromHm ‘Poised Promoter’ classification in the GM12878 cell-line [54]. A
463 random set of 500bp windows representing an equivalent CpG density distribution of the feature set in question
464 were selected from the genome-wide data. The number of windows selected in each permutation for these features
465 was; for tRNAs 1,320, for bivalent chromatin 42,841 and for polycomb group protein target promoters 13,502.
466 Above a certain CpG density there are insufficient windows to sample without replacement within a permutation.
467 Furthermore, above $\sim \geq 18\%$ CpG density CpG Islands become consistently hypomethylated [109]. Therefore, all
468 windows with a CpG density of $\geq 18\%$ (45 CpGs per 500bp) were grouped and sampled from the same pool.
469 i.e. a window overlapping a tRNA gene which had a 20% density could be represented in permutation by one
470 with any density $\geq 18\%$. This permutation was performed 1,000 times to determine an Empirical p value by
471

calculating the number of times the permutation result exceeded the observed number of significant windows in
472 the feature set. *Empirical p – value* = $\frac{r+1}{N+1}$, where r is the sum of significant windows in all permutations and N
473 is number of permutations [110].
474

Neonate and Centenarian Whole Genome Bisulfite Sequencing

475

DNA methylation calls were downloaded from GEO: GSE31263 and intersected with tRNA genes using bedtools
476 v2.17.0 [106].
477

Sample pooling and EPIC array

478

We performed an Illumina Infinium DNA methylation EPIC array ((C) Illumina) and targeted bisulfite
479 sequencing of select tRNA gene loci. Here we used DNA extracted from whole blood and pooled into 8 samples
480 from unrelated individuals at 4 time-points with 2 pools at each time-point. The timepoints were 4, 28, 63, and
481 78 years. Using the EPIC array we were able to infer the DNAm age using the Horvath DNAm clock [11] and
482 blood cell-type composition of our samples using the Houseman algorithm [51], as implemented in the **meffil**
483 v1.1.1 R package using the 'blood gse35069' cell type reference option [111].
484

Targeted Bisulfite Sequencing

485

We selected tRNA loci for targeted sequencing in which have had observed changes and DNAm with age and
486 closely related tRNAs in which changes were not observed. Primer design was performed using 'methPrimer' v1
487 [112] (Supplementary Data 7). A total of 84 tRNA loci were targeted and 79 subsequently generated reliable
488 results post-QC. The targeted tRNAs covered a total of 723 CpGs with a median of 8 CpGs per tRNA (range
489 1-13), data passing QC was generated for 458 CpGs, median 6 (range 1-9) per tRNA.
490

Quality was assessed before and after read trimming using **fastqc** v0.11.5 [113] and **multiqc** v1.0 [114] to
491 visualise the results. Targeting primers were trimmed with **cutadapt** v1.13 [115] and a custom **per15** script.
492 Quality trimming was performed with **trim_galore** 0.5.0 [115]. Alignment and methylation calling was
493 performed with **Bismark** v0.20.0 [117] making use of **bowtie2** v2.3.1 [118]. The alignment was performed against
494 both the whole hg19 genome and just the tRNA genes +/- 100bp to assess the possible impact of off-target
495 mapping. Mapping to the whole genome did produce purported methylation calls at a larger number of loci than
496 mapping just to the tRNA genes (683,783 vs 45,861 respectively). Introducing a minimum coverage threshold of
497 25 reads dramatically reduced this and brought the number of sites into line with that in the tRNA gene set
498 (36,065 vs 33,664 respectively) suggesting a small number of ambiguously mapping reads. All subsequent analysis
499 was performed using the alignment to just the tRNA genes with a minimum coverage of 25 reads.
500

We performed pairwise differential methylation analysis of the tRNA genes at the different time points using 501
RnBeads v2.0.1 [52] with limma v3.38.3 [119] and a minimum coverage of 25 reads. We also performed linear 502
regression predicting age from DNA methylation at the targeted tRNA sites, permitting us to compare rates of 503
increase with age. For the linear regression, we used only CpG sites with more than 25 reads mapped to the 504
regions of the genome targeted for amplification. 505

TwinsUK Illumina 450k array methylomes 506

Illumina Infinium DNA methylation 450k arrays ((C) Illumina) were also performed on TwinsUK participants, in 507
770 Blood-derived DNA samples which had matched MeDIP-seq data. These data were preprocessed in the form 508
of methylation ‘beta’ values pre-processed as previously described [16,107]. Cell-type correction was performed 509
using cell-count data and the following model: lm(age ~ beta + eosinophils + lymphocytes + monocytes 510
+ neutrophils). 511

Chromatin Segmentation Data 512

Epilogos chromatin segmentation data [53] was downloaded for the tRNA gene regions +/- 200bp from 513
https://explore.altius.org/tabix/epilogos/hg19.15.Blood_T-cell.KL.gz using the tabix v1.3.2 utility. 514
The data used was the ‘Blood & T-cell’ 15 State model based on segmentation of 14 cell-types. This data was 515
manipulated and visualised with R v3.5.2 and ggplot2 v3.2.1. 516

Isolated Blood Cell Type Specific Data 517

Data from 7 cell-type fractions from 6 Male individuals was downloaded from GSE35069 [55] using GEOquery 518
v2.51.5 [119]. Five of the 6 top age hypermethylating tRNAs are covered by this array dataset. Heatmaps were 519
created with the ComplexHeatmap v1.20.0 R package [56]. 520

Cancer and Tissue Specific Methylation Data 521

Data was downloaded from the TCGA (The Cancer Genome Atlas) via the GDC (genomic data commons) data 522
portal [121] using the GenomicDataCommons R package v1.6.0. Data from foetal tissue [61,62] was downloaded 523
from GEO (GSE72867, GSE30654). From the TCGA, we selected samples for which DNAm data was available 524
from both the primary site and normal solid tissue, and for which we could infer an approximate age (within one 525
year). We selected those probes overlapping tRNA genes yielding 73,403 data points across 19 tissues with an age 526
range of 15-90yrs (median 63.4) (Supplementary Data 8) 527

Mouse RRBS Analysis

We downloaded methylation calls and coverage information resulting from RRBS performed by Petkovich *et al.* [63] from GEO using GEOquery v2.51.5 [119] GSE80672. These data from 152 mice covered 68 tRNA and 436 CpGs after QC requiring >50 reads per CpG and >10 data points per tRNA. We excluded 5 tRNAs from blacklisted regions of mm10 [46]. After QC there were 58 tRNA genes and 385 CpGs. We performed simple linear modeling to predict age from methylation level at each tRNA and each CpG.

Data Availability Statement

All data used in this study is publicly available under the following accession numbers.

Targeted Bisulfite sequencing data is deposited in the sequence read archive with the bioproject accession: PRJNA635108 [<https://www.ncbi.nlm.nih.gov/bioproject/PRJNA635108>]

EPIC array data is deposited at GEO with the accession: GSE166503
[<https://www.ncbi.nlm.nih.gov/geo/query/acc.cgi?acc=GSE166503>]

Neonate and Centenarian Whole Genome Bisulfite Sequencing DNA methylation calls: GSE31263
[<https://www.ncbi.nlm.nih.gov/geo/query/acc.cgi?acc=GSE31263>].

Human isolated blood cell-type specific DNA methylation array Data: GSE35069
[<https://www.ncbi.nlm.nih.gov/geo/query/acc.cgi?acc=GSE35069>].

Cancer and tissue specific DNA methylation array data from TCGA, see (Supplementary) for the full list of samples drawn from genomic data commons.

Feotal tissue DNA methylation data were downloaded from: GSE72867
[<https://www.ncbi.nlm.nih.gov/geo/query/acc.cgi?acc=GSE72867>], & GSE30654
[<https://www.ncbi.nlm.nih.gov/geo/query/acc.cgi?acc=GSE30654>].

Mouse whole blood RRBS DNA methylation data data: GSE80672
[<https://www.ncbi.nlm.nih.gov/geo/query/acc.cgi?acc=GSE80672>].

The MeDIP-seq data supporting the results of this article are available in the EMBL-EBI European Genome-phenome Archive (EGA) under Data set Accession number EGAD00010000983
[<https://www.ebi.ac.uk/ega/datasets/EGAD00010000983>], access is subject to request and approval by their Data Access Committee.

epilogos chromatin segmentation data is available from:
[https://explore.altius.org/tabix/epilogos/hg19.15.Blood_T-cell.KL.gz]

Twins UK DNA metylation and age model summary data for non-overlapping 500bp windows is available at

via UCSC Genome Browser's track hub interface, add: <http://epigenome.soton.ac.uk/TrackHub/hub.txt> Tracks 558
include: mean, median and variance in RPM values across all samples in the model (n = 3001); the percentage of 559
samples with an exactly 0 RPM score in a given window (useful for spotting technical issues); the slope and 560
-log10(p-values) for batch corrected, and blood cell-type corrected age models. 561

tRNA gene annotations for the hg19 and mm10 genomes were acquired from GtRNAdb 562
[<http://gtrnadb.ucsc.edu/>] 563

Source data for all figures are provided with this paper. 564

Code availability

Available at https://github.com/RichardJActon/tRNA_paper_code 565

<https://doi.org/10.5281/zenodo.4294046> [122] 566

Acknowledgements

568

We gratefully acknowledge the individuals from TwinsUK, Mavidos and the Hertfordshire cohort. TwinsUK received funding from the Wellcome Trust (Ref: 081878/Z/06/Z), European Community's Seventh Framework Programme (FP7/2007-2013), the National Institute for Health Research (NIHR)-funded BioResource, Clinical Research Facility and Biomedical Research Centre based at Guy's and St Thomas' NHS Foundation Trust in partnership with King's College London. Further funding support for the EpiTwin project was obtained from the European Research Council (project number 250157) and BGI. SNP Genotyping was performed by The Wellcome Trust Sanger Institute and National Eye Institute via NIH/CIDR. The authors would like to thank Nikki Graham for her assistance with the identification and pooling of the MAVIDOS and Hertfordshire DNA samples. The authors also acknowledge the use of the IRIDIS High Performance Computing Facility, and associated support services at the University of Southampton, in the completion of this work. The MRC-LEU is supported by the Medical Research Council (MRC). RJA was in receipt of a MRC Doctoral fund (1820097).

569

570

571

572

573

574

575

576

577

578

579

Author Contributions

580

RJA designed experiments and analysed all the processed and experimental data. CGB conceived and designed the experiments. TDS and JW conceived and provided TwinsUK MeDIP-seq data. YX, FG and JW produced raw MeDIP-seq data with WY and JB processing and quality controlling these data. WY contributed an analysis concept. CC, NCH, ED, and KL provided MAVIDOS and Hertfordshire sample data. EB, EW, and CAM performed the targeted BiS sequencing experiment. PGH contributed additional data and discussion of results. RJA and CGB wrote the paper. All authors reviewed and approved the final manuscript.

581

582

583

584

585

586

Competing Interests

587

CC has received lecture fees and honoraria from Amgen, Danone, Eli Lilly, GSK, Kyowa Kirin, Medtronic, Merck, Nestle, Novartis, Pfizer, Roche, Servier, Shire, Takeda and UCB outside of the submitted work. NCH reports personal fees, consultancy, lecture fees and honoraria from Alliance for Better Bone Health, AMGEN, MSD, Eli Lilly, Servier, Shire, UCB, Consilient Healthcare, Kyowa Kirin and Internis Pharma, outside the submitted work. ED has received speaker/consultancy fees from Pfizer, UCB and Lilly. TDS is a consultant to Zoe Global Ltd ('Zoe'). All other authors declare no competing interests.

588

589

590

591

592

593

References

594

1. Partridge L, Deelen J, Slagboom PE. Facing up to the global challenges of ageing. *Nature*. Springer US; 2018;561: 45–56. doi:10.1038/s41586-018-0457-8 595
2. Campisi J, Kapahi P, Lithgow GJ, Melov S, Newman JC, Verdun E. From discoveries in ageing research to 596 therapeutics for healthy ageing. *Nature*. Springer US; 2019;571: 183–192. doi:10.1038/s41586-019-1365-2 597
3. López-Otín C, Blasco MA, Partridge L, Serrano M, Kroemer G. The hallmarks of aging. *Cell*. 2013;153: 600 1194–217. doi:10.1016/j.cell.2013.05.039
4. Booth LN, Brunet A. The aging epigenome. *Molecular Cell*. Elsevier Inc.; 2016;62: 728–744. 601 doi:10.1016/j.molcel.2016.05.013
5. Wilson VL, Jones PA. DNA methylation decreases in aging but not in immortal cells. *Science* (New York, 602 NY). 1983;220: 1055–7. Available: <http://www.ncbi.nlm.nih.gov/pubmed/6844925> 603
6. Fraga MF, Ballestar E, Paz MF, Ropero S, Setien F, Ballestar ML, et al. From the cover: Epigenetic 604 differences arise during the lifetime of monozygotic twins. *Proceedings of the National Academy of Sciences*. 605 2005;102: 10604–10609. doi:10.1073/pnas.0500398102
7. Chuong EB, Elde NC, Feschotte C. Regulatory activities of transposable elements: From conflicts to 606 benefits. *Nature Reviews Genetics*. Nature Publishing Group; 2017;18: 71–86. doi:10.1038/nrg.2016.139 607
8. Teschendorff AE, Menon U, Gentry-Maharaj A, Ramus SJ, Weisenberger DJ, Shen H, et al. Age-dependent 608 DNA methylation of genes that are suppressed in stem cells is a hallmark of cancer. *Genome research*. 609 2010;20: 440–6. doi:10.1101/gr.103606.109
9. Rakyan VK, Down TA, Maslau S, Andrew T, Yang TP, Beyan H, et al. Human aging-associated DNA 610 hypermethylation occurs preferentially at bivalent chromatin domains. *Genome Research*. 2010;20: 434–439. 611 doi:10.1101/gr.103101.109
10. Hannum G, Guinney J, Zhao L, Zhang L, Hughes G, Sadda S, et al. Genome-wide methylation profiles 612 reveal quantitative views of human aging rates. *Molecular cell*. Elsevier Inc.; 2013;49: 359–367. 613 doi:10.1016/j.molcel.2012.10.016
11. 614

- Horvath S. DNA methylation age of human tissues and cell types. *Genome biology*. 2013;14: R115. doi:10.1186/gb-2013-14-10-r115 616
12.
- Weidner CI, Lin Q, Koch CM, Eisele L, Beier F, Ziegler P, et al. Aging of blood can be tracked by DNA methylation changes at just three CpG sites. *Genome biology*. 2014;15: R24. doi:10.1186/gb-2014-15-2-r24 617
13.
- Bell CG, Lowe R, Adams PD, Baccarelli AA, Beck S, Bell JT, et al. DNA methylation aging clocks: Challenges and recommendations. *Genome biology*. 2019;20: 249. doi:10.1186/s13059-019-1824-y 618
14.
- Horvath S, Raj K. DNA methylation-based biomarkers and the epigenetic clock theory of ageing. *Nature Reviews Genetics*. Springer US; 2018;19: 371–384. doi:10.1038/s41576-018-0004-3 619
15.
- Field AE, Robertson NA, Wang T, Havas A, Ideker T, Adams PD. DNA methylation clocks in aging: Categories, causes, and consequences. *Molecular Cell*. Elsevier Inc.; 2018;71: 882–895. doi:10.1016/j.molcel.2018.08.008 620
16.
- Bell CG, Xia Y, Yuan W, Gao F, Ward K, Roos L, et al. Novel regional age-associated DNA methylation changes within human common disease-associated loci. *Genome Biology*. 2016;17: 193. doi:10.1186/s13059-016-1051-8 621
17.
- Rideout EJ, Marshall L, Grewal SS. Drosophila RNA polymerase III repressor Maf1 controls body size and developmental timing by modulating tRNA^{iMet} synthesis and systemic insulin signaling. *Proceedings of the National Academy of Sciences*. 2012;109: 1139–1144. doi:10.1073/pnas.1113311109 622
18.
- Kolitz SE, Lorsch JR. Eukaryotic initiator tRNA: Finely tuned and ready for action. *FEBS Letters*. 2010;584: 396–404. doi:10.1016/j.febslet.2009.11.047 623
19.
- Pavon-Eternod M, Gomes S, Rosner MR, Pan T. Overexpression of initiator methionine tRNA leads to global reprogramming of tRNA expression and increased proliferation in human epithelial cells. *RNA*. 2013;19: 461–466. doi:10.1261/rna.037507.112 624
20.
- Eigen M, Lindemann B, Tietze M, Winkler-Oswatitsch R, Dress A, Haeseler A von. How old is the genetic code? Statistical geometry of tRNA provides an answer. *Science*. 1989;244: 673–679. doi:10.1126/science.2497522 625
21.
- Tavernarakis N. Ageing and the regulation of protein synthesis: A balancing act? *Trends in Cell Biology*. 2008;18: 228–235. doi:10.1016/j.tcb.2008.02.004 626

22. Pliatsika V, Loher P, Magee R, Telonis AG, Londin E, Shigematsu M, et al. MINTbase v2.0: A 637 comprehensive database for tRNA-derived fragments that includes nuclear and mitochondrial fragments from all the cancer genome atlas projects. *Nucleic Acids Research*. Oxford University Press; 2018;46: D152–D159. doi:10.1093/nar/gkx1075
23.
- Schimmel P. The emerging complexity of the tRNA world: Mammalian tRNAs beyond protein synthesis. 638 Nature reviews Molecular cell biology. Nature Publishing Group; 2018;19: 45–58. doi:10.1038/nrm.2017.77
24.
- Lee YS, Shibata Y, Malhotra A, Dutta A. A novel class of small RNAs: tRNA-derived RNA fragments 641 (tRFs). *Genes & development*. 2009;23: 2639–49. doi:10.1101/gad.1837609
25.
- Li S, Xu Z, Sheng J. tRNA-derived small RNA: A novel regulatory small non-coding RNA. *Genes*. 2018;9: 642 246. doi:10.3390/genes9050246
26.
- Xu W-L, Yang Y, Wang Y-D, Qu L-H, Zheng L-L. Computational approaches to tRNA-derived small 644 RNAs. *Non-Coding RNA*. 2017;3: 2. doi:10.3390/ncrna3010002
27.
- Chan PP, Lowe TM. GtRNAd: A database of transfer RNA genes detected in genomic sequence. *Nucleic 646 acids research*. 2009;37: D93–7. doi:10.1093/nar/gkn787
28.
- Parisien M, Wang X, Pan T. Diversity of human tRNA genes from the 1000-genomes project. *RNA Biology*. 648 2013;10: 1853–1867. doi:10.4161/rna.27361
29.
- Lodish H, Berk A, Zipursky SL, Matsudaira P, Baltimore D, Darnell J. Molecular cell biology, 4th edition 650 [Internet]. 4th ed. New York: W. H. Freeman; 2000. Available: <https://www.ncbi.nlm.nih.gov/books/NBK21475/>
30.
- Schramm L. Recruitment of RNA polymerase III to its target promoters. *Genes & Development*. 2002;16: 652 2593–2620. doi:10.1101/gad.1018902
31.
- Canella D, Praz V, Reina JH, Cousin P, Hernandez N. Defining the RNA polymerase III transcriptome: 654 Genome-wide localization of the RNA polymerase III transcription machinery in human cells. *Genome research*. 2010;20: 710–21. doi:10.1101/gr.101337.109
32.

- Besser D, Götz F, Schulze-Forster K, Wagner H, Kröger H, Simon D. DNA methylation inhibits transcription by RNA polymerase III of a tRNA gene, but not of a 5S rRNA gene. FEBS letters. 1990;269: 358–62.
doi:10.1016/0014-5793(90)81193-R
33. 658
- Varshney D, Vavrova-Anderson J, Oler AJ, Cowling VH, Cairns BR, White RJ. SINE transcription by RNA polymerase III is suppressed by histone methylation but not by DNA methylation. Nature communications. Nature Publishing Group; 2015;6: 6569. doi:10.1038/ncomms7569
34. 659
- Murawski M, Szczesniak B, Zoladek T, Hopper AK, Martin NC, Boguta M. maf1 mutation alters the subcellular localization of the Mod5 protein in yeast. Acta biochimica Polonica. 1994;41: 441–8. Available:
<http://www.ncbi.nlm.nih.gov/pubmed/7732762>
35. 660
- Pluta K, Lefebvre O, Martin NC, Smagowicz WJ, Stanford DR, Ellis SR, et al. Maf1p, a negative effector of RNA polymerase III in *saccharomyces cerevisiae*. Molecular and Cellular Biology. 2001;21: 5031–5040.
doi:10.1128/MCB.21.15.5031-5040.2001
36. 661
- Mange F, Praz V, Migliavacca E, Willis IM, Schütz F, Hernandez N. Diurnal regulation of RNA polymerase III transcription is under the control of both the feeding–fasting response and the circadian clock. Genome Research. 2017;27: 973–984. doi:10.1101/gr.217521.116
37. 662
- Kennedy BK, Lamming DW. The mechanistic target of rapamycin: The grand ConducTOR of metabolism and aging. Cell Metabolism. Elsevier Inc.; 2016;23: 990–1003. doi:10.1016/j.cmet.2016.05.009
38. 663
- Nwanaji-Enwerem JC, Weisskopf MG, Baccarelli AA. Multi-tissue DNA methylation age: Molecular relationships and perspectives for advancing biomarker utility. Ageing Research Reviews. Elsevier; 2018;45: 15–23. doi:10.1016/j.arr.2018.04.005
39. 664
- Hansen M, Taubert S, Crawford D, Libina N, Lee S-J, Kenyon C. Lifespan extension by conditions that inhibit translation in *caenorhabditis elegans*. Aging Cell. 2007;6: 95–110. doi:10.1111/j.1474-9726.2006.00267.x
40. 665
- Filer D, Thompson MA, Takhayev V, Dobson AJ, Kotronaki I, Green JWM, et al. RNA polymerase III limits longevity downstream of TORC1. Nature. Nature Publishing Group; 2017;552: 263–267.
doi:10.1038/nature25007
41. 666

- Dhahbi JM, Spindler SR, Atamna H, Yamakawa A, Boffelli D, Mote P, et al. 5' tRNA halves are present as abundant complexes in serum, concentrated in blood cells, and modulated by aging and calorie restriction. BMC Genomics. 2013;14: 298. doi:10.1186/1471-2164-14-298
42. 676
- Zhou W, Laird PW, Shen H. Comprehensive characterization, annotation and innovative use of infinium DNA methylation BeadChip probes. Nucleic Acids Research. 2016;45: gkw967. doi:10.1093/nar/gkw967
43. 677
- Van Bortle K, Phanstiel DH, Snyder MP. Topological organization and dynamic regulation of human tRNA genes during macrophage differentiation. Genome Biology. Genome Biology; 2017;18: 180. doi:10.1186/s13059-017-1310-3
44. 678
- Down TA, Rakyan VK, Turner DJ, Flicek P, Li H, Kulesha E, et al. A bayesian deconvolution strategy for immunoprecipitation-based DNA methylome analysis. Nature Biotechnology. 2008;26: 779–785. doi:10.1038/nbt1414
45. 679
- Lowe TM, Chan PP. tRNAscan-SE on-line: Integrating search and context for analysis of transfer RNA genes. Nucleic Acids Research. 2016;44: W54–W57. doi:10.1093/nar/gkw413
46. 680
- Amemiya HM, Kundaje A, Boyle AP. The ENCODE blacklist: Identification of problematic regions of the genome. Scientific Reports. 2019;9: 9354. doi:10.1038/s41598-019-45839-z
47. 681
- Geiger H, Haan G de, Florian MC. The ageing haematopoietic stem cell compartment. Nature Reviews Immunology. Nature Publishing Group; 2013;13: 376–389. doi:10.1038/nri3433
48. 682
- Ziller MJ, Gu H, Müller F, Donaghey J, Tsai LT-Y, Kohlbacher O, et al. Charting a dynamic DNA methylation landscape of the human genome. Nature. 2013;500: 477–81. doi:10.1038/nature12433
49. 683
- Christensen BC, Houseman EA, Marsit CJ, Zheng S, Wrensch MR, Wiemels JL, et al. Aging and environmental exposures alter tissue-specific DNA methylation dependent upon CpG island context. Schübeler D, editor. PLoS Genetics. 2009;5: e1000602. doi:10.1371/journal.pgen.1000602
50. 684
- Heyn H, Li N, Ferreira HJ, Moran S, Pisano DG, Gomez A, et al. Distinct DNA methylomes of newborns and centenarians. Proceedings of the National Academy of Sciences. 2012;109: 10522–10527. doi:10.1073/pnas.1120658109
51. 685

- Houseman EA, Accomando WP, Koestler DC, Christensen BC, Marsit CJ, Nelson HH, et al. DNA methylation arrays as surrogate measures of cell mixture distribution. *BMC Bioinformatics*. 2012;13: 86. doi:10.1186/1471-2105-13-86
52. Müller F, Scherer M, Assenov Y, Lutsik P, Walter J, Lengauer T, et al. RnBeads 2.0: Comprehensive analysis of DNA methylation data. *Genome Biology*. *Genome Biology*; 2019;20: 55. doi:10.1186/s13059-019-1664-9
53. Meuleman W. Epilogos [Internet]. 2019. Available: <https://epilogos.altius.org/>
54. Ernst J, Kheradpour P, Mikkelsen TS, Shresh N, Ward LD, Epstein CB, et al. Mapping and analysis of chromatin state dynamics in nine human cell types. *Nature*. 2011;473: 43–49. doi:10.1038/nature09906
55. Reinius LE, Acevedo N, Joerink M, Pershagen G, Dahlén S-E, Greco D, et al. Differential DNA methylation in purified human blood cells: Implications for cell lineage and studies on disease susceptibility. Ting AH, editor. *PLoS ONE*. 2012;7: e41361. doi:10.1371/journal.pone.0041361
56. Gu Z, Eils R, Schlesner M. Complex heatmaps reveal patterns and correlations in multidimensional genomic data. *Bioinformatics*. 2016;32: 2847–2849. doi:10.1093/bioinformatics/btw313
57. Schmitt BM, Rudolph KLM, Karagianni P, Fonseca NA, White RJ, Talianidis I, et al. High-resolution mapping of transcriptional dynamics across tissue development reveals a stable mRNA–tRNA interface. *Genome Research*. 2014;24: 1797–1807. doi:10.1101/gr.176784.114
58. Dittmar KA, Goodenbour JM, Pan T. Tissue-specific differences in human transfer RNA expression. *PLoS genetics*. 2006;2: e221. doi:10.1371/journal.pgen.0020221
59. Sagi D, Rak R, Gingold H, Adir I, Maayan G, Dahan O, et al. Tissue- and time-specific expression of otherwise identical tRNA genes. Chisholm AD, editor. *PLOS Genetics*. 2016;12: e1006264. doi:10.1371/journal.pgen.1006264
60. Slieker RC, Iterson M van, Luijk R, Beekman M, Zhernakova DV, Moed MH, et al. Age-related accrual of methylomic variability is linked to fundamental ageing mechanisms. *Genome biology*. *Genome Biology*; 2016;17: 191. doi:10.1186/s13059-016-1053-6
61.

- Yang Z, Wong A, Kuh D, Paul DS, Rakyan VK, Leslie RD, et al. Correlation of an epigenetic mitotic clock with cancer risk. *Genome Biology*. *Genome Biology*; 2016;17: 205. doi:10.1186/s13059-016-1064-3
716
62.
- Nazor KL, Altun G, Lynch C, Tran H, Harness JV, Slavin I, et al. Recurrent variations in DNA methylation in human pluripotent stem cells and their differentiated derivatives. *Cell Stem Cell*. 2012;10: 620–634.
717
doi:10.1016/j.stem.2012.02.013
63.
- Petkovich DA, Podolskiy DI, Lobanov AV, Lee S-G, Miller RA, Gladyshev VN. Using DNA methylation profiling to evaluate biological age and longevity interventions. *Cell Metabolism*. 2017;25: 954–960.e6.
718
doi:10.1016/j.cmet.2017.03.016
64.
- Thornlow BP, Armstrong J, Holmes AD, Howard JM, Corbett-Detig RB, Lowe TM. Predicting transfer RNA gene activity from sequence and genome context. *Genome Research*. 2020;30: 85–94.
719
doi:10.1101/gr.256164.119
65.
- Ehrlich M. DNA hypermethylation in disease: Mechanisms and clinical relevance. *Epigenetics*. Taylor & Francis; 2019;14: 1141–1163. doi:10.1080/15592294.2019.1638701
720
66.
- Xu Z, Taylor JA. Genome-wide age-related DNA methylation changes in blood and other tissues relate to histone modification, expression and cancer. *Carcinogenesis*. 2014;35: 356–364. doi:10.1093/carcin/bgt391
721
67.
- Slieker RC, Relton CL, Gaunt TR, Slagboom PE, Heijmans BT. Age-related DNA methylation changes are tissue-specific with ELOVL2 promoter methylation as exception. *Epigenetics and Chromatin*. BioMed Central; 2018;11: 1–11. doi:10.1186/s13072-018-0191-3
722
68.
- Zhu T, Zheng SC, Paul DS, Horvath S, Teschendorff AE. Cell and tissue type independent age-associated DNA methylation changes are not rare but common. *Aging*. 2018;10: 3541–3557.
723
doi:10.18632/aging.101666
69.
- Lappalainen T, Greally JM. Associating cellular epigenetic models with human phenotypes. *Nature Reviews Genetics*. Nature Publishing Group; 2017;18: 441–451. doi:10.1038/nrg.2017.32
724
70.
- Moskowitz DM, Zhang DW, Hu B, Le Saux S, Yanes RE, Ye Z, et al. Epigenomics of human CD8 t cell differentiation and aging. *Science Immunology*. 2017;2: eaag0192. doi:10.1126/sciimmunol.aag0192
725
71.

- Hashimoto K, Kouno T, Ikawa T, Hayatsu N, Miyajima Y, Yabukami H, et al. Single-cell transcriptomics reveals expansion of cytotoxic CD4 t cells in supercentenarians. *Proceedings of the National Academy of Sciences of the United States of America*. 2019;116: 24242–24251. doi:10.1073/pnas.1907883116
72. 736
- Goodenbour JM, Pan T. Diversity of tRNA genes in eukaryotes. *Nucleic acids research*. 2006;34: 6137–46.
73. doi:10.1093/nar/gkl725
73. 737
- Keam SP, Young PE, McCorkindale AL, Dang THY, Clancy JL, Humphreys DT, et al. The human piwi protein Hiwi2 associates with tRNA-derived piRNAs in somatic cells. *Nucleic Acids Research*. 2014;42:
8984–8995. doi:10.1093/nar/gku620
74. 740
- Geslain R, Pan T. Functional analysis of human tRNA isodecoders. *Journal of Molecular Biology*. 2010;396:
821–831. doi:10.1016/j.jmb.2009.12.018
75. 742
- Kirchner S, Cai Z, Rauscher R, Kastelic N, Anding M, Czech A, et al. Alteration of protein function by
a silent polymorphism linked to tRNA abundance. Hurst L, editor. *PLOS Biology*. 2017;15: e2000779.
doi:10.1371/journal.pbio.2000779
76. 744
- Li S, Shi X, Chen M, Xu N, Sun D, Bai R, et al. Angiogenin promotes colorectal cancer metastasis via
tiRNA production. *International Journal of Cancer*. 2019; ijc.32245. doi:10.1002/ijc.32245
77. 746
- Kim HK, Fuchs G, Wang S, Wei W, Zhang Y, Park H, et al. A transfer-RNA-derived small RNA regulates
ribosome biogenesis. *Nature*. Nature Publishing Group; 2017;552: 57–62. doi:10.1038/nature25005
78. 748
- Martinez G, Choudury SG, Slotkin RK. tRNA-derived small RNAs target transposable element transcripts.
Nucleic Acids Research. 2017;45: 5142–5152. doi:10.1093/nar/gkx103
79. 750
- Torres AG, Reina O, Stephan-Otto Attolini C, Ribas de Pouplana L. Differential expression of human
tRNA genes drives the abundance of tRNA-derived fragments. *Proceedings of the National Academy of
Sciences*. 2019;116: 201821120. doi:10.1073/pnas.1821120116
80. 752
- Gu P, Jia S, Takasugi T, Smith E, Nandakumar J, Hendrickson E, et al. CTC1-STN1 coordinates g- and
c-strand synthesis to regulate telomere length. *Aging Cell*. 2018;17: e12783. doi:10.1111/acel.12783
81. 754
- Wang Y, Brady KS, Caiello BP, Ackerson SM, Stewart JA. Human CST suppresses origin licensing and
promotes AND-1/Ctf4 chromatin association. *Life Science Alliance*. 2019;2: e201800270.
doi:10.26508/lsa.201800270
82. 756

82. Sargolzaeiaval F, Zhang J, Schleit J, Lessel D, Kubisch C, Precioso DR, et al. CTC1 mutations in a
757
brazilian family with progeroid features and recurrent bone fractures. *Molecular Genetics & Genomic*
758
Medicine.
83. 2018;6: 1148–1156. doi:10.1002/mgg3.495
- Gomez-Roman N, Grandori C, Eisenman RN, White RJ. Direct activation of RNA polymerase III
759
transcription by c-Myc. *Nature.* 2003;421: 290–294. doi:10.1038/nature01327
- 84.
- Crighton D. p53 represses RNA polymerase III transcription by targeting TBP and inhibiting promoter
760
occupancy by TFIIIB. *The EMBO Journal.* 2003;22: 2810–2820. doi:10.1093/emboj/cdg265
- 85.
- Sutcliffe JE, Brown TRP, Allison SJ, Scott PH, White RJ. Retinoblastoma protein disrupts interactions
761
required for RNA polymerase III transcription. *Molecular and Cellular Biology.* 2000;20: 9192–9202.
762
doi:10.1128/MCB.20.24.9192-9202.2000
- 86.
- Schmitt BM, Rudolph KLM, Karagianni P, Fonseca NA, White RJ, Talianidis I, et al. High-resolution
763
mapping of transcriptional dynamics across tissue development reveals a stable mRNA-tRNA interface.
764
Genome research. 2014;24: 1797–807. doi:10.1101/gr.176784.114
- 87.
- Gerber A, Ito K, Chu C-S, Roeder RG. Gene-specific control of tRNA expression by RNA polymerase II.
765
Molecular Cell. Elsevier Inc.; 2020;78: 765–778.e7. doi:10.1016/j.molcel.2020.03.023
- 88.
- Gingold H, Tehler D, Christoffersen NR, Nielsen MM, Asmar F, Kooistra SM, et al. A dual program for
766
translation regulation in cellular proliferation and differentiation. *Cell.* Elsevier Inc.; 2014;158: 1281–1292.
767
doi:10.1016/j.cell.2014.08.011
- 89.
- Rudolph KLM, Schmitt BM, Villar D, White RJ, Marioni JC, Kutter C, et al. Codon-driven translational
768
efficiency is stable across diverse mammalian cell states. Galtier N, editor. *PLoS genetics.* 2016;12:
769
e1006024. doi:10.1371/journal.pgen.1006024
- 90.
- Gingold H, Dahan O, Pilpel Y. Dynamic changes in translational efficiency are deduced from codon usage
770
of the transcriptome. *Nucleic acids research.* 2012;40: 10053–63. doi:10.1093/nar/gks772
- 91.
- Thornlow BP, Hough J, Roger JM, Gong H, Lowe TM, Corbett-Detig RB. Transfer RNA genes experience
771
exceptionally elevated mutation rates. *Proceedings of the National Academy of Sciences.* 2018;115:
772
8996–9001. doi:10.1073/pnas.1801240115
- 92.

- Iben JR, Maraia RJ. tRNA gene copy number variation in humans. *Gene*. 2014;536: 376–384. 778
doi:10.1016/j.gene.2013.11.049
93. 779
- Darrow EM, Chadwick BP. A novel tRNA variable number tandem repeat at human chromosome 1q23.3 780
is implicated as a boundary element based on conservation of a CTCF motif in mouse. *Nucleic Acids* 781
Research. 2014;42: 6421–6435. doi:10.1093/nar/gku280
94. 782
- Huang S, Sun B, Xiong Z, Shu Y, Zhou H, Zhang W, et al. The dysregulation of tRNAs and tRNA 783
derivatives in cancer. *Journal of Experimental & Clinical Cancer Research. Journal of Experimental &* 784
Cancer Research; 2018;37: 101. doi:10.1186/s13046-018-0745-z
95. 785
- Krishnan P, Ghosh S, Wang B, Heyns M, Li D, Mackey JR, et al. Genome-wide profiling of transfer RNAs 786
and their role as novel prognostic markers for breast cancer. *Scientific Reports*. Nature Publishing Group; 787
2016;6: 32843. doi:10.1038/srep32843
96. 788
- Müller CA, Nieduszynski CA. DNA replication timing influences gene expression level. *The Journal of* 789
Cell Biology. 2017;216: 1907–1914. doi:10.1083/jcb.201701061
97. 790
- Du Q, Bert SA, Armstrong NJ, Caldon CE, Song JZ, Nair SS, et al. Replication timing and epigenome 791
remodelling are associated with the nature of chromosomal rearrangements in cancer. *Nature Communications*. 792
Springer US; 2019;10: 416. doi:10.1038/s41467-019-08302-1
98. 793
- Cruickshanks HA, McBryan T, Nelson DM, VanderKraats ND, Shah PP, Tuyn J van, et al. Senescent cells 794
harbour features of the cancer epigenome. *Nature Cell Biology*. 2013;15: 1495–1506. doi:10.1038/ncb2879
99. 795
- Hamdani O, Dhillon N, Hsieh T-HS, Fujita T, Ocampo J, Kirkland JG, et al. tRNA genes affect 796
chromosome structure and function via local effects. *Molecular and cellular biology*. 2019;39: 1–26.
doi:10.1128/MCB.00432-18
100. 797
- Raab JR, Chiu J, Zhu J, Katzman S, Kurukuti S, Wade PA, et al. Human tRNA genes function as chromatin 798
insulators. *The EMBO journal*. Nature Publishing Group; 2012;31: 330–50. doi:10.1038/emboj.2011.406
101. 799
- Noma K, Cam HP, Maraia RJ, Grewal SIS. A role for TFIIIC transcription factor complex in genome 800
organization. *Cell*. 2006;125: 859–72. doi:10.1016/j.cell.2006.04.028
102. 801
- Sun L, Yu R, Dang W. Chromatin architectural changes during cellular senescence and aging. *Genes*. 802
2018;9: 211. doi:10.3390/genes9040211
803. 804

103. Moayyeri A, Hammond CJ, Valdes AM, Spector TD. Cohort profile: TwinsUK and healthy ageing twin study. International Journal of Epidemiology. 2013;42: 76–85. doi:10.1093/ije/dyr207 799
104. Harvey NC, Javaid K, Bishop N, Kennedy S, Papageorgiou AT, Fraser R, et al. MAVIDOS maternal vitamin d osteoporosis study: Study protocol for a randomized controlled trial. The MAVIDOS study group. Trials. 2012;13: 13. doi:10.1186/1745-6215-13-13 800
105. Syddall H, Aihie Sayer A, Dennison E, Martin H, Barker D, Cooper C. Cohort profile: The hertfordshire cohort study. International Journal of Epidemiology. 2005;34: 1234–1242. doi:10.1093/ije/dyi127 801
106. Quinlan AR, Hall IM. BEDTools: A flexible suite of utilities for comparing genomic features. Bioinformatics. 802
- University of Utah; 2010;26: 841–842. doi:10.1093/bioinformatics/btq033 803
107. Bell CG, Gao F, Yuan W, Roos L, Acton RJ, Xia Y, et al. Obligatory and facilitative allelic variation in the DNA methylome within common disease-associated loci. Nature Communications. 2018;9: 8. doi:10.1038/s41467-017-01586-1 804
108. Lienhard M, Grimm C, Morkel M, Herwig R, Chavez L. MEDIPS: Genome-wide differential coverage analysis of sequencing data derived from DNA enrichment experiments. Bioinformatics. 2014;30: 284–286. doi:10.1093/bioinformatics/btt650 805
109. Bell CG, Wilson GA, Butcher LM, Roos C, Walter L, Beck S. Human-specific CpG "beacons" identify loci associated with human-specific traits and disease. Epigenetics. 2012;7: 1188–99. doi:10.4161/epi.22127 806
110. North BV, Curtis D, Sham PC. A note on the calculation of empirical p values from monte carlo procedures. The American Journal of Human Genetics. 2003;72: 498–499. doi:10.1086/346173 807
111. Min J. L., Hemani G., Davey Smith G., Relton C., Suderman M. Meffil: efficient normalization and analysis of very large DNA methylation datasets. Bioinformatics. 2018;18: 1427–31. Available: <https://www.ncbi.nlm.nih.gov/pmc/articles/PMC6247925/> 808
112. Li L-C, Dahiya R. MethPrimer: Designing primers for methylation PCRs. Bioinformatics (Oxford, England). 2002;23: 3983–89. Available: <http://www.ncbi.nlm.nih.gov/pubmed/12424112> 809
113. Andrews S. FastQC [Internet]. Cambridge: Babraham Bioinformatics; 2010. Available: <http://www.bioinformatics.babraham.ac.uk/projects/fastqc> 810

114. Ewels P, Magnusson M, Lundin S, Käller M. MultiQC: Summarize analysis results for multiple tools and samples in a single report. *Bioinformatics* (Oxford, England). 2016;32: 3047–8. doi:10.1093/bioinformatics/btw354 821
115. Martin M. Cutadapt removes adapter sequences from high-throughput sequencing reads. *EMBnetjournal*. 2011;17: 10. doi:10.14806/ej.17.1.200 822
116. Krueger F. Trim galore [Internet]. 2015. Available: https://www.bioinformatics.babraham.ac.uk/projects/trim_galore/ 823
117. Krueger F, Andrews SR. Bismark: A flexible aligner and methylation caller for bisulfite-seq applications. *Bioinformatics*. 2011;27: 1571–1572. doi:10.1093/bioinformatics/btr167 824
118. Langmead B, Salzberg SL. Fast gapped-read alignment with bowtie 2. *Nature Methods*. 2012;9: 357–359. doi:10.1038/nmeth.1923 825
119. Ritchie ME, Phipson B, Wu D, Hu Y, Law CW, Shi W, et al. Limma powers differential expression analyses for RNA-sequencing and microarray studies. *Nucleic Acids Research*. 2015;43: e47–e47. doi:10.1093/nar/gkv007 826
120. Sean D, Meltzer PS. GEOquery: A bridge between the gene expression omnibus (GEO) and BioConductor. *Bioinformatics*. 2007;23: 1846–1847. doi:10.1093/bioinformatics/btm254 827
121. Grossman RL, Heath AP, Ferretti V, Varmus HE, Lowy DR, Kibbe WA, et al. Toward a shared vision for cancer genomic data. *New England Journal of Medicine*. 2016;375: 1109–1112. doi:10.1056/NEJMmp1607591 828
122. Acton RJ, Bourne E, Bell J, Lillycrop K, Wang J, Dennison E, et al. [Code for] the genomic loci of specific human tRNA genes exhibit ageing-related DNA hypermethylation. 2020. doi:10.5281/zenodo.4294046 829

Supplementary Information

839

Supplementary Figures

840

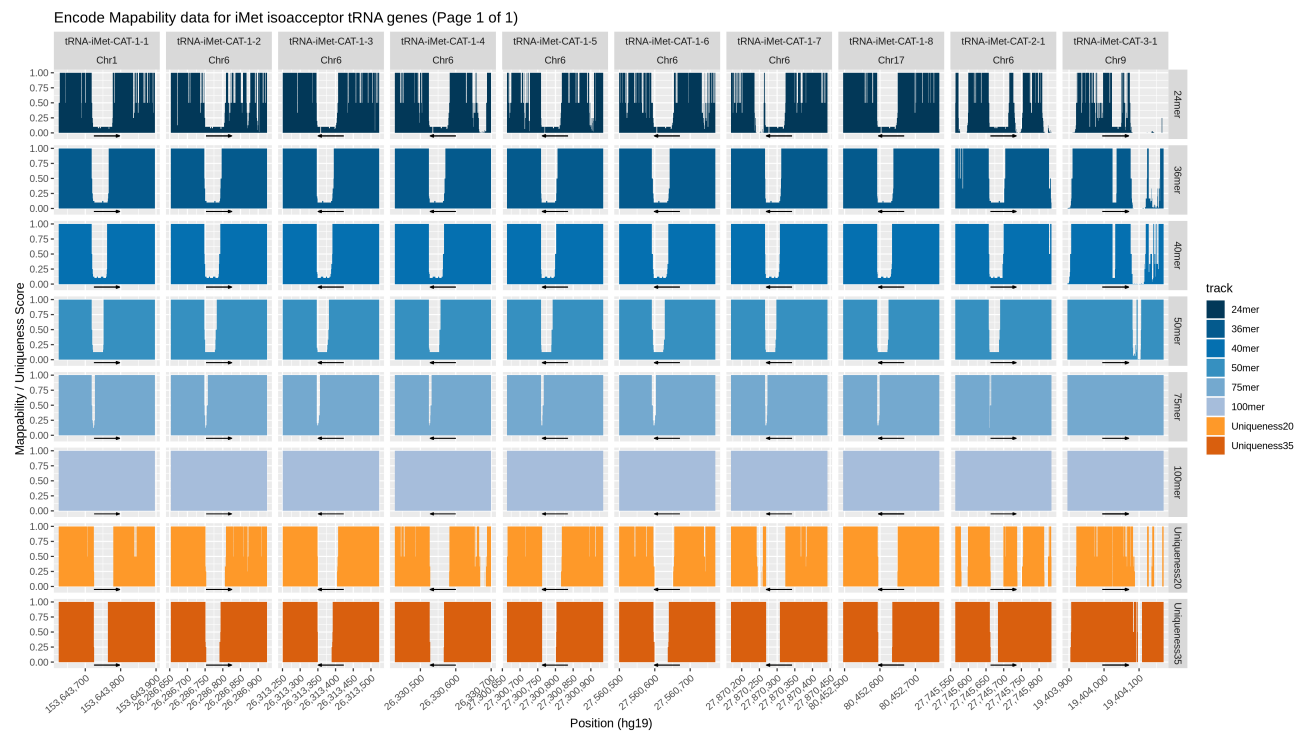


Figure Supplementary Figure 1. Example of mappability data from the encode mappability tracks [123] for the initiator methionine tRNA genes. Source data are provided as a Source Data file.

tRNA mappability

tRNA region only Vs tRNA +/- 500bp

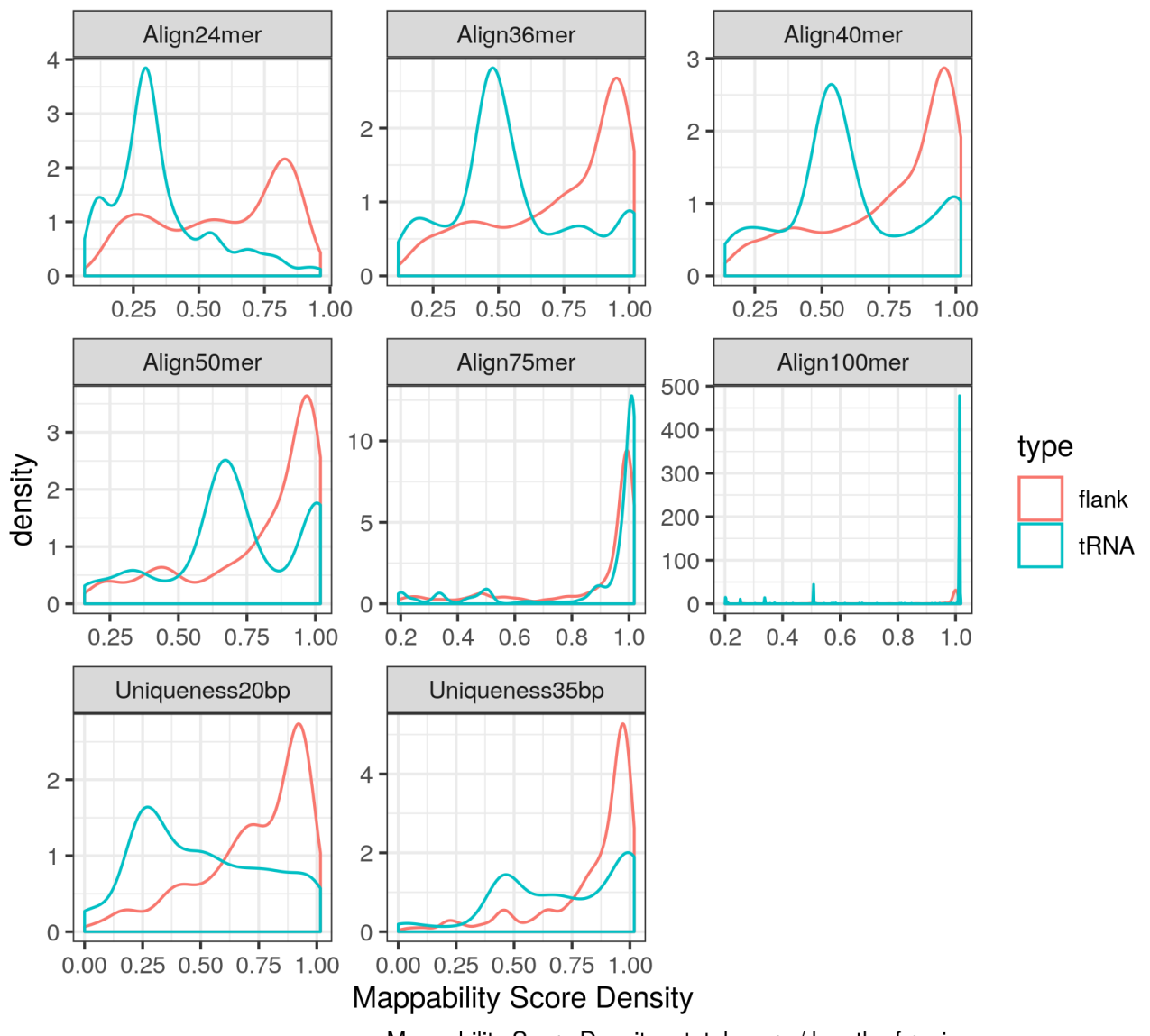


Figure Supplementary Figure 2. Mappability score density of the tRNA genes increases with read length and is greater when flanking regions ($\pm 500\text{bp}$) are included. Mappability score density is computed as the area under the encode mappability tracks [123] over the length of the region. Source data are provided as a Source Data file.

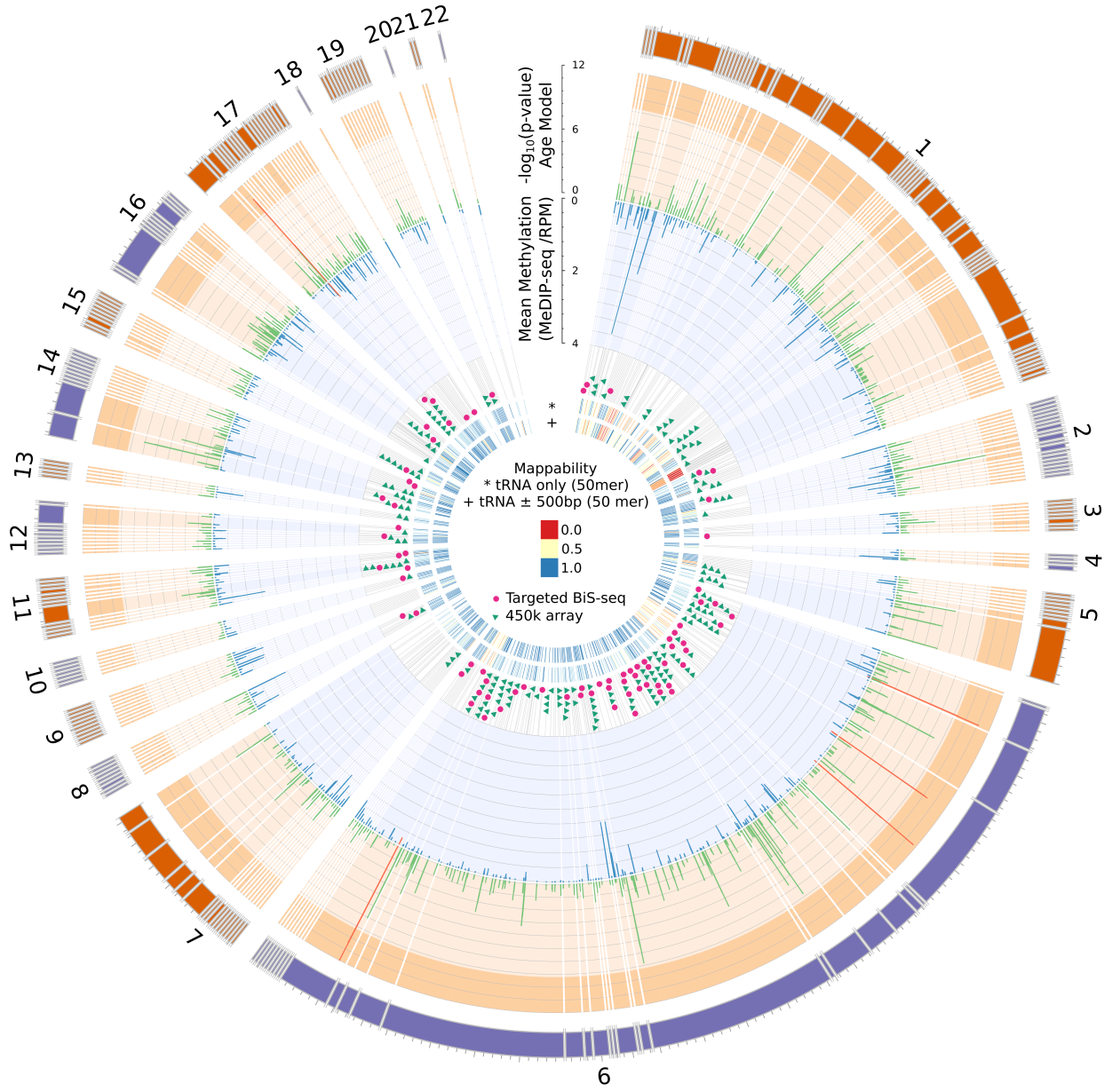


Figure Supplementary Figure 3. Human tRNA genes overview. From the outside in: Chromosome ideograms scaled by the number of tRNA genes (total = 598), as excludes chromosome X (10), Y (0) and contig chr1_gl000192_random (2; see Methods). tRNA genes within 20kbp of one another are grouped with breaks inserted between these clusters. Radial grey lines represent the location of tRNA genes in the genome. $-\log_{10}(p - \text{value})$ for the blood cell-type and batch corrected age model are shown for each window overlapping a tRNA gene in green. Mean methylation across all samples ($n=3001$) in RPM (reads per million base pairs) is shown in blue. Genome-wide significant cell-type & batch corrected ($p < 4.34 \times 10^{-9}$) tRNAs show in red. The 158 Loci covered by 213 probes on the 450k array which directly overlap a tRNA gene are shown with green triangles. The 84 loci targeted for bisulfite sequencing in this study are indicated in magenta. Mappability score density is computed as the area under the encode mappability tracks [123] over the length of the region.

Mean methylation by tRNA Sorted Blood Cell-types (GSE35069)

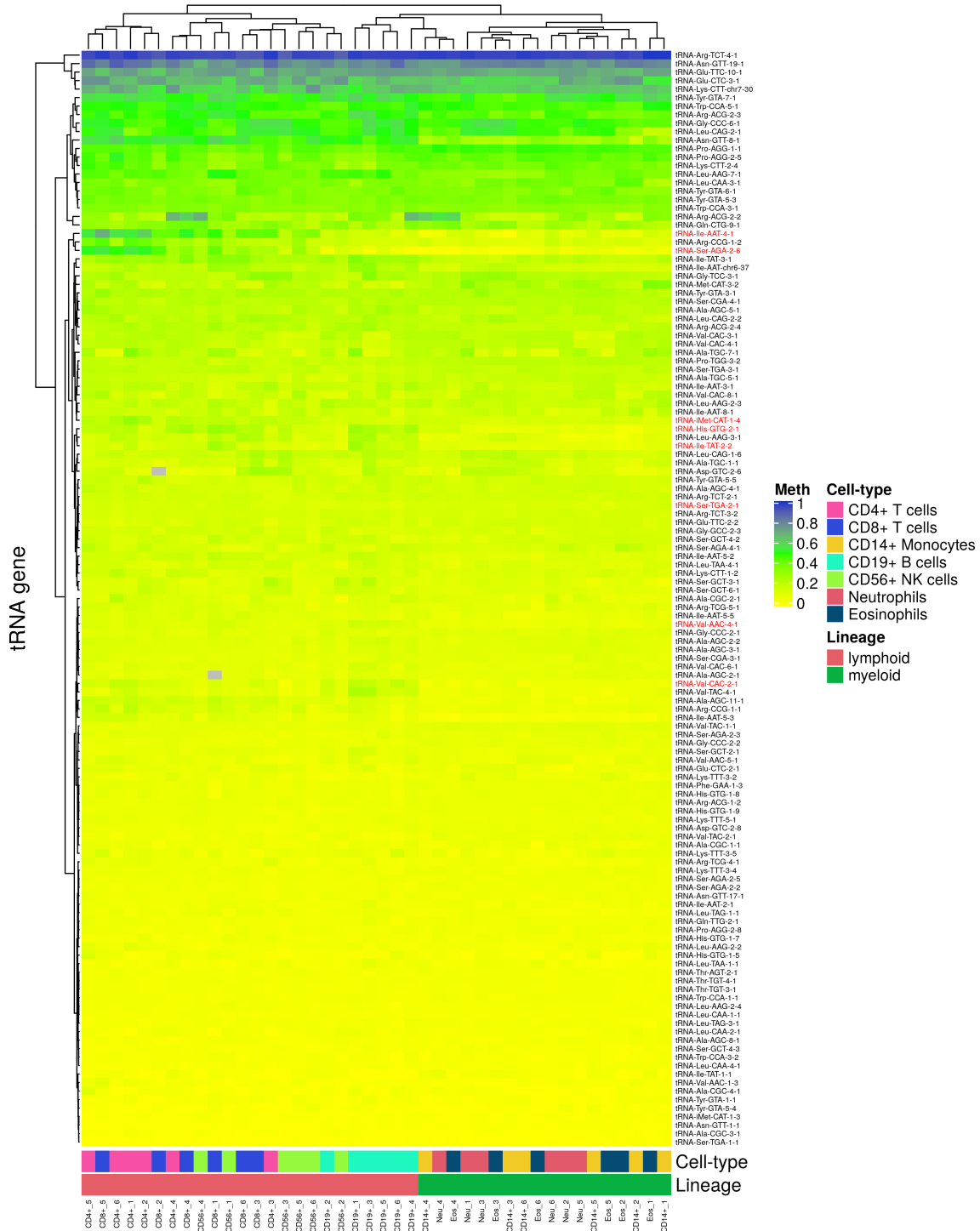


Figure Supplementary Figure 4. Heatmap Mean Methylation of probes covering each tRNA in 7 cell-type fractions from 6 Male individuals. Showing all 150 tRNAs covered by 213 probes on the Illumina 450k array. Data from GSE35069 [55] downloaded using GEOquery [56,119]. Source data are provided as a Source Data file.

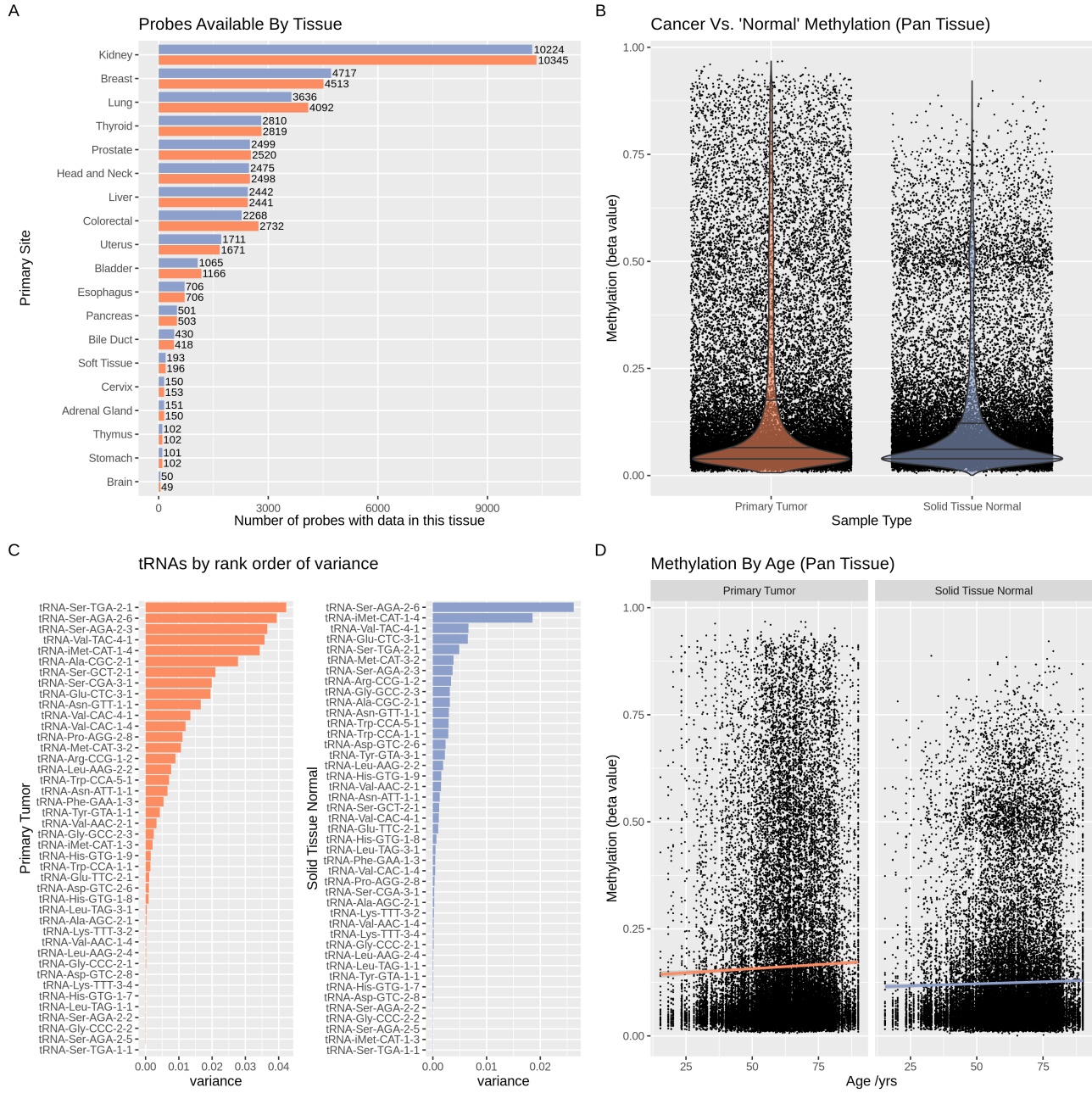


Figure Supplementary Figure 5. Global properties of tRNA methylation data for 45 tRNA genes across 19 tissues with matched normal and tumour samples from 733 cases in TCGA [61,62]. The horizontal lines in the violin plots represent the 25%, 50% and 75% quantiles. a) Number of DNA methylation array probes with available data by primary site tissue type for normal tissue and primary tumour samples, b) DNA methylation level distribution for normal tissue and primary tumour site samples, c) Variance in DNA methylation levels by tRNA for normal tissue and primary tumour site samples, d) DNA methylation levels by age in normal tissue and primary tumour site samples, Source data are provided as a Source Data file.

Mean methylation by tRNA In Solid Tissue Normal Samples

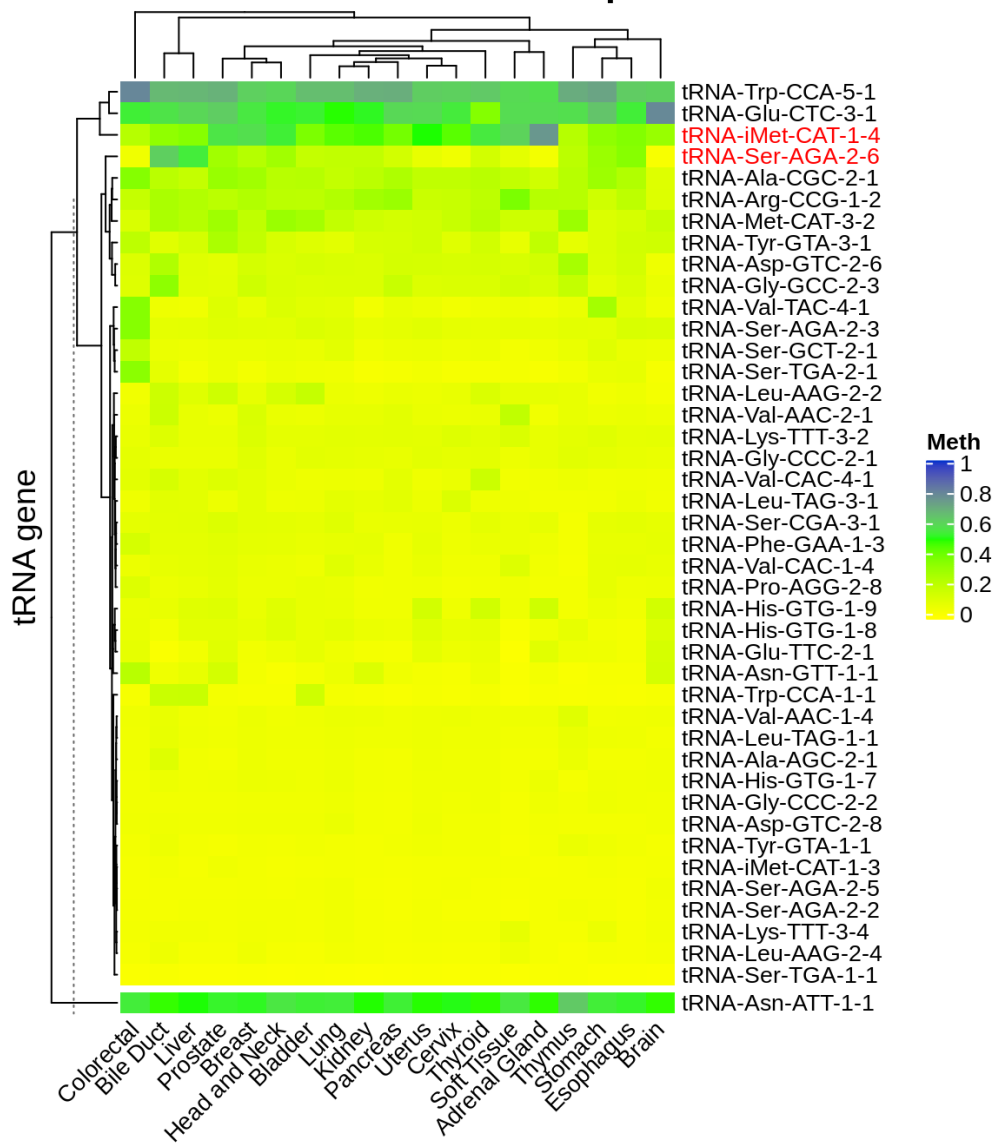


Figure Supplementary Figure 6. Mean Methylation of 43 tRNAs in 19 tissues. Possible pseudogene (tRNA-Asn-ATT-1-1) is shown in a separate cluster beneath the main heatmap [56]. Source data are provided as a Source Data file.

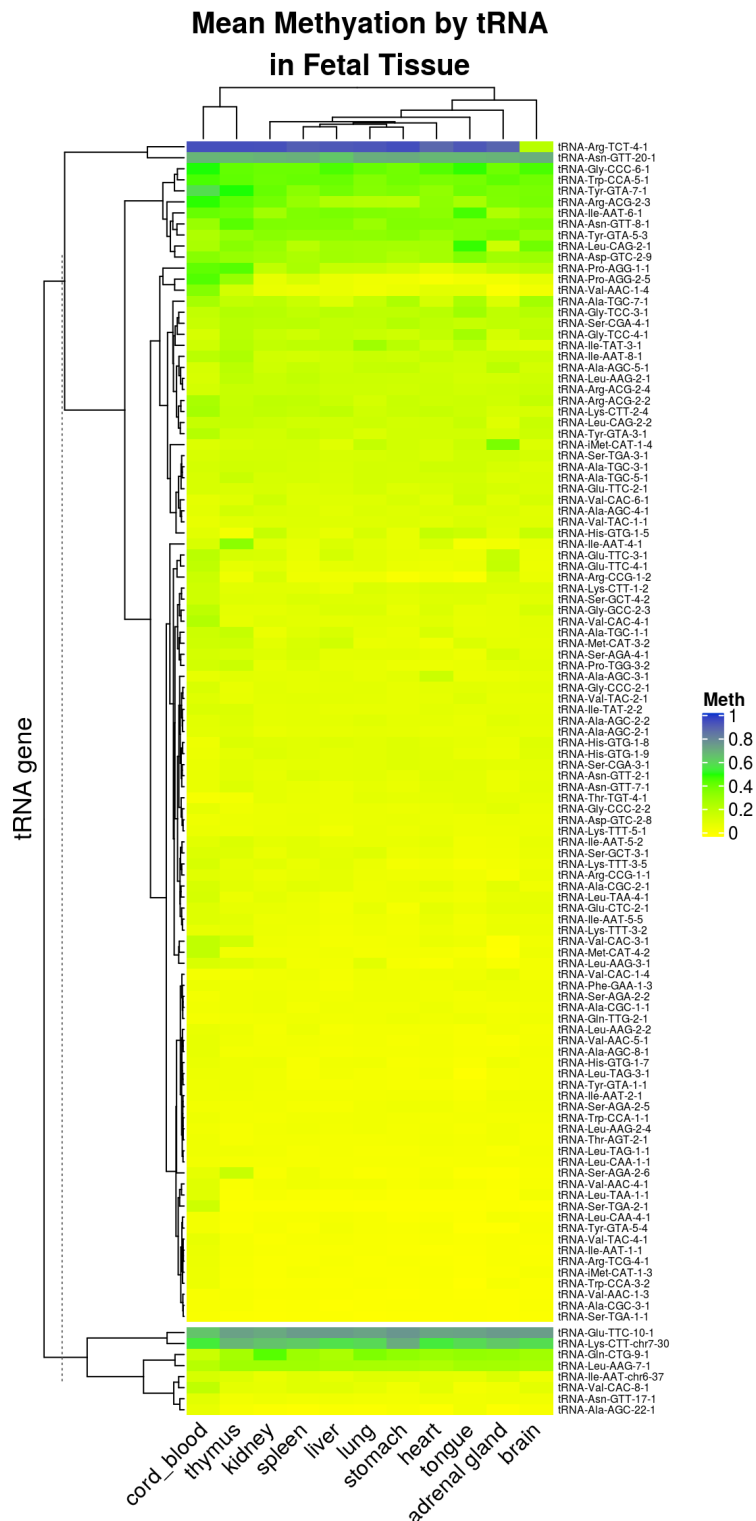


Figure Supplementary Figure 7. Mean Methylation of 115 tRNAs in 11 tissues. Possible pseudogenes are shown in a separate cluster beneath the main heatmap [56]. Source data are provided as a Source Data file.

CpG Density in tRNA Regions

Compared to non-tRNA regions within 5kb of tRNA genes

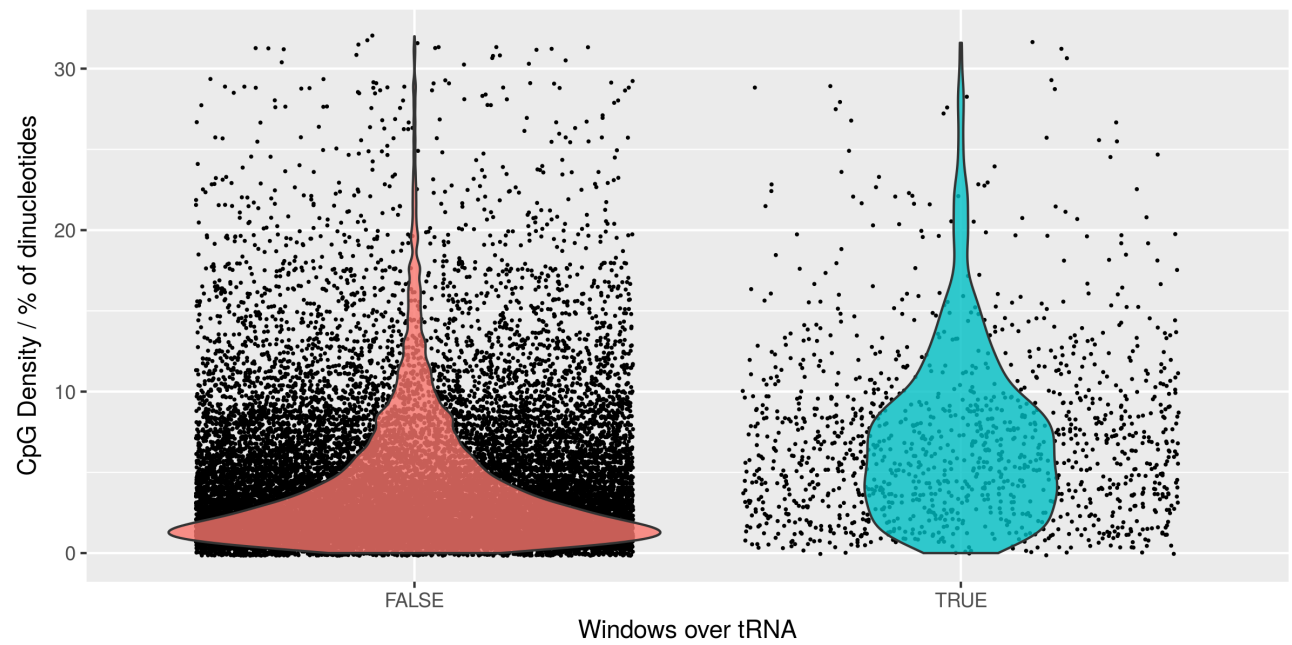


Figure Supplementary Figure 8. CpG Density in windows overlapping tRNA genes compared to that of non-tRNA overlapping windows in flanking sequences (+/-5kb)

tRNA gene cluster numbers by bin size

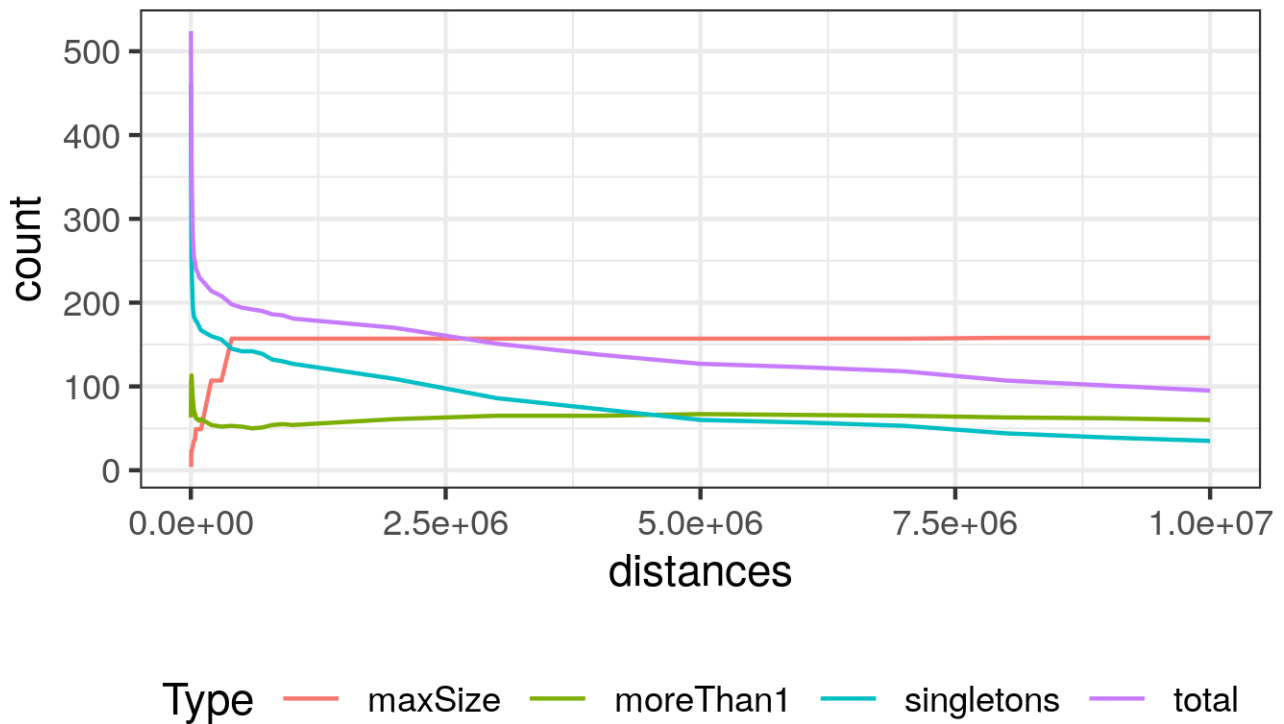


Figure Supplementary Figure 9. tRNA gene cluster numbers at different bin sizes total: total number of tRNA clusters. singletons: number of tRNAs in clusters alone. moreThan1: number of tRNAs in clusters with more than one tRNA. maxSize: the number of tRNAs in the largest cluster. Source data are provided as a Source Data file.